Design and Simulation of a PI-Controlled Step-Up DC–DC Converter for Precise Voltage Regulation

Submitted By

Md. Rakibul Hasan Roni	**ID: EEE2201025068**
Khairun Naher	**ID: EEE2201025013**
Md. Sumon Hossain	**ID: EEE2201025015**
Md. Shohanur Rahman Sazzad	**ID: EEE2201025090**
Md. Foysal Ahmmed Fahim	**ID: EEE2201025042**

Supervised By

Soikot Sarkar

Lecturer, Department of EEE
Sonargaon University

Department of Electrical and Electronic Engineering
Sonargaon University (SU)
147/1, Panthapath
Dhaka-1215

Date of Submission: September.2025

DECLARATION

We hereby declare that we have a declared that the work presented in this thesis is the outcome of the investigation performed by us under the supervision of **Soikot Sorker,** Lecturer of the Electrical and Electronic Engineering Department, Sonargaon University. We also declare that the work contained in this thesis has not been previously submitted to meet requirements for an award at this or any other higher education institution. To the best of my knowledge and belief, the Thesis contains no material previously published or written by another person except where due reference is cited. Furthermore, the Thesis complies with **PLAGIARISM** and **ACADEMIC INTEGRITY** regulation of Sonargaon University.

Md. Rakibul Hasan Roni
ID: EEE2201025068

Khairun Naher
ID: EEE2201025013

Md. Sumon Hossain
ID: EEE2201025015

Md. Shohanur Rahman Sazzad
ID: EEE2201025090

Md. Foysal Ahmmed Fahim
ID: EEE2201025042

CERTIFICATION

This is to certify that the thesis report **"DESIGN AND SIMULATION OF A PI-CONTROLLED STEP-UP DC–DC CONVERTER FOR PRECISE VOLTAGE REGULATION"** is the confide record of the work done by- **Md. Rakibul Hasan Roni (EEE2201025068) , Khairun Naher (EEE2201025013), Md. Sumon Hossain (EEE2201025015), Md. Shohanur Rahman Sazzad (EEE2201025090), Md. Foysal Ahmmed Fahim (EEE2201025042)**

For partial fullfilment and of the requirement of the degree BSc. in Electrical and Electronics Engineering at Sonargaon University,
The thesis report has been carried out under my guidance and is a confide record of the successful work. I wish success in future.

Supervised By

Soikot Sarkar

Lecturer, Department of EEE
Sonargaon University

Acknowledgement

First and foremost, all praise and thanks to the **Almighty Allah** for granting us the strength, patience, and opportunity to complete our thesis.

We would like to express our deepest gratitude to our respected supervisor, **Soikot Sarkar** for his continuous support, invaluable guidance, and constant encouragement throughout the course of this research. His patience, insightful feedback, and dedication to teaching have inspired us more than words can express.

We thank each other for the teamwork, collaboration, and endless discussions that made this journey both productive and memorable.

we would also like to express our thanks to the respected head of EEE dept. **Md. Rais Uddin Mollah** for providing us the opportunity to conduct our research in such an academic environment

Finally, we would like to thank our parents and families for their unconditional love, endless prayers, and unwavering belief in us. Their emotional and moral support has been the foundation of our perseverance.

.

Abstract

This study presents a DC-DC boost converter using a Proportional-Integral (PI) controller for efficient voltage regulation where a 60 V input was utilized to obtain a stable 110 V output with fast response, low ripple, and high stability under load variations. The numerical calculation was carried out by employing MATLAB/Simulink with continuous conduction mode (CCM) approach where the values of the fundamental components including the inductor, capacitor, and load resistor were considered based on a 400 W design specification. The PI controller was tuned using the Simulink PID tuner to optimize system performance where final tuned gains, Kp=0.023954 and Ki=8.2609 delivered excellent dynamic results with a rise time of 0.0459 s, a settling time of 0.0746 s, and an overshoot of only 0.361%. The steady state duty cycle reached 0.46, matching theoretical expectations. Moreover, the output voltage ripple was maintained within 0.1%, and inductor current remained steady around 6.85 A, confirming operation in CCM. Error-based performance metrics, including IAE, ISE, ITAE, MAE, and MSE all showed negligible values, indicating high control accuracy.

Table of Contents

Abstract iv
Table of Contents v
List of Figures vii
List of Tables ix
Chapter 1: INTRODUCTION 1
1.1 Background 1
1.2 Aims and Objectives 2
1.3 Significance, Scope and Definitions 3
1.4 Thesis Outline 3
Chapter 2: LITERATURE REVIEW 5
2.1 Introduction 5
2.2 Previous Studies 5
2.3 Summary and Implications 15
Chapter 3: METHODOLOGY 17
3.1 Overview of the Research Approach 17
3.2 Mathematical Modelling of the Boost Converter 18
3.3 Calculation of Design Parameters 21
3.3.1 DESIGN SPECIFICATION 22
3.3.2 PARAMETER CALCULATION 22
3.4 PI Controller Design and Tuning 25
3.5 Simulation Environment and Model Setup 28
3.6 Definition of Performance Metrics 29
3.6.1 Time-Domain Performance Metrics 29
3.6.2 Error-Based Performance Metrics 30
3.7 Simulation Execution and Data Acquisition 31
Chapter 4: RESULTS ANALYSIS AND DISCUSSION 32
4.1 PI Controller Tuning Results 32
4.2 Simulation Output 33
4.2.1 Output Voltage Waveforms (PI Tuned) 33
4.2.2 Inductor Current Profiles 35
4.2.3 Duty Cycle Profile 38
4.3 Performance Metrics 40
4.4 Impact of different parameters in boost converter 42
4.5 Effect of Inductance Variation on System Performance Parameters 46
4.6 Effect of Resistance Variation on System Performance Parameters 48

4.7 Effect of Capacitance Variation on System Performance Parameters 51
4.8 Effect of Frequency Variation on System Performance Parameters 52
4.9 Summary 54
Chapter 5: CONCLUSIONS 56
5.1 Key Findings 56
5.2 Limitation of the Study 56
5.3 PRACTICAL Implication 57
5.4 Recommendation for Further Study 57
Bibliography 59
Appendix 63
1. Matlab code for calculating the design parameters values 63
2. Maltab Code for Calculating the performance metrics values 63

List of Figures

Fig. No. **Figure Caption** **Page No.**

Figure 2.1: Proposed PI controller-based DC-DC Boost converter by Adnan et al. [19].....6

Figure 2.2: Proposed PI Controller structure [23]. 6

Figure 2.3: Simulation model proposed by [24]. 8

Figure 2.4: Block diagram of the designed model by [25]. 8

Figure 2.5: Simulation of the PI controller boost converter by [26].....9

Figure 2.6: Sliding mode structure designed by [27].....10

Figure 2.7: Dual loop control of Boost converter design [29]. 11

Figure 2.8: Proposed system designed by Lenine et al. [30]. 12

Figure 2.9: Controller block diagram [31]. 12

Figure 2.10: Three port converter system [32]. 14

Figure 2.11: Hardware setup of the proposed system [33]. 15

Figure 3.1: Flowchart of the overall workflow. 18

Figure 3.2: Typical Boost converter circuit [24]. 19

Figure 3.3: Operation of the converter when in Mode I [24]. 20

Figure 3.4: Operation of the converter when in Mode II [24]. 20

Figure 3.5: The converter's control system structured with PI controller in a closed-loop configuration. 26

Figure 3.6: PI Tuner using the Transfer Function Based automated tuning. 27

Figure 3.7: Boost converter with PI controller SIMULINK model. 29

Figure 4.1: Input and output voltage graph from the Boost converter. 34

Figure 4.2: Output Graph signal statistics after settling the final value. 35

Figure 4.3: Inductor Current Graph. 36

Figure 4.4: Inductor Current Signal Statistics. 37

Figure 4.5: Generated PWM signal for MOSFET. 38

Figure 4.6: Duty Cycle Graph of the Tuned PI controller. 39

Figure 4.7. Impact of other parameters of boost converter with respect to Vin. 42

Figure 4.8. Impact of other parameters of boost converter with respect to Vout. 43

Figure 4.9. Impact of other parameters of boost converter with respect to D. 45

Figure 4.10. Impact of other parameters of boost converter with respect to Fs. 46

Figure 4.11. Effect of changing inductor on the system performance. 47

Figure 4.12. Effect of changing resistance on the system performance. 49
Figure 4.13. Effect of changing capacitance on the system performance. 51
Figure 4.14. Effect of changing frequency on the system performance. 54

List of Tables

Table No. **Table Caption** **Page No.**

Table 3.1: Design specification and final Calculated Parameters for the Boost Converter. 25

Table 4.1: Summary of The PI Tuning Results. 32

Table 4.2: Summary results of the performance metrics. 40

Table 4.3. Data on the impact of inductance variation on boost converter performance 48

Table 4.4. Data on the impact of resistance variation on boost converter performance 50

Table 4.5. Data on the impact of capacitance variation on boost converter performance 52

Table 4.6. Data on the Impact of Frequency Variation on Boost Converter Performance. 53

Chapter 1: INTRODUCTION

1.1 BACKGROUND

DC-DC boost converters are widely used in modern power electronics systems where the higher output voltage is needed from the lower input source. These converters are found in many applications such as renewable energy systems, battery charging circuits, electric vehicles, LED drivers, and portable electronic devices [1]. In all these systems, the converter plays a key role by stepping up the voltage level while keeping the system efficient and responsive [2-5]. Like in a solar power system, the voltage from a solar panel is not always stable. It depends on sunlight, temperature, and weather conditions. This voltage must be raised to a constant level before it is used or stored in a battery. Similarly, in electric vehicles, the converter steps up the battery voltage to run motors or charge auxiliary units. These systems require the boost converter to deliver stable, accurate, and fast voltage control under all working conditions [6]. However, during operation, the output voltage of the converter may not always remain stable. Changes in input voltage or load demand can cause the output to drop or overshoot. If not controlled properly, this can affect the performance of the entire system and may damage sensitive electronics [7]. Therefore, an effective control strategy is necessary for keeping the output voltage near to the desired reference at all times. Among many control strategies, the PI controller is the most common solutions. It is used widely because of its simple structure, low cost, and good reliability [8]. The PI controller works by comparing the output voltage with a reference voltage. If there is any error, it changes the duty cycle of the converter's switch to correct the output. In this way, the controller keeps the voltage stable [9]. However, the performance of the PI controller depends heavily on the correct selection of its two gain parameters: the proportional gain (K_p) and

the integral gain (K_i) [10]. If these gains are not chosen properly, the converter may show slow response, overshoot, high ripple, or instability. On the other hand, when the gains are tuned correctly, the PI controller can provide excellent voltage regulation, fast response to disturbances, and smooth steady-state operation [11]. With proper tuning, the PI controller can meet performance targets like low overshoot, short settling time, and minimal voltage ripple. Because of these advantages, the PI controller remains a strong choice for DC-DC boost converters, especially when tuned carefully. This thesis aims to design and simulate a boost converter system using a well-tuned PI controller. The focus is on achieving good voltage regulation, fast transient performance, and high efficiency, even under varying input and load conditions. This research will explore the tuning process, system modeling, and testing in simulation to show how the PI controller can deliver stable and reliable performance in real-world scenarios.

1.2 AIMS AND OBJECTIVES

The aim of the project is to design a DC–DC boost converter with well-tuned PI controller to deliver stable, efficient, and responsive voltage output.

Objectives:

- To model a boost converter system with 60 V input and 110 V output.
- To calculate design values for inductor, capacitor, and resistor based on design specification.
- To use MATLAB/Simulink for PI controller tuning using a transfer function–based method.
- To minimize common performance errors such as IAE (Integrated Absolute Error), ISE (Integrated Square Error), and ITAE (Integrated Time Absolute Error).

- To observe improvements in overshoot, settling time, and ripple using tuned PI gains.

1.3 SIGNIFICANCE, SCOPE AND DEFINITIONS

This research is important as of many real-world systems depend on boost converters to deliver clean and stable power. Additionally, a poorly controlled converter may caused system failure or reduce overall efficiency. While PI controllers are widely used in practice, many systems still rely on basic tuning methods that do not give the best performance. This study fills that gap by using a proper tuning process, based on the converter's transfer function and system parameters. MATLAB/Simulink is used to simulate and analyse the converter, which makes the testing more accurate and detailed. The scope of the study is limited to simulation only. The converter is designed for 400 W power, 60 V input, and 110 V output, operating in continuous conduction mode. Hardware implementation and external disturbances such as temperature changes or switching losses are not covered in this work. Some key terms used in this study include: PI Controller, which adjusts the output by using proportional and integral gains; Duty Cycle, which refers to the ratio of the ON time of the switch to the total switching period; Ripple, which means small voltage or current fluctuations; Transfer Function, which is a mathematical model of the system used for tuning; and IAE, ISE, ITAE, which are different ways to measure how well the system performs over time.

1.4 THESIS OUTLINE

This thesis is structured into five main chapters.

Chapter 1 provides the introduction, including background, aims and objectives, significance, and the thesis layout.

Chapter 2 presents a detailed literature review on previous works related to boost converter design and PI controller applications. It highlights the methods used by researchers and identifies the gaps that this study aims to address.

Chapter 3 explains the methodology used in designing the boost converter system. It includes the calculation of component values such as the inductor, capacitor, and resistor. It also describes how the PI controller is tuned using MATLAB/Simulink tools and explains how the system is tested under different conditions.

Chapter 4 presents the simulation results, showing how the converter behaves. It includes values for performance metrics such as IAE, ISE, ITAE, MAE, and MSE, and discusses the system's voltage regulation and transient behavior.

Chapter 5 concludes the study by summarizing the main findings, discussing the limitations, and giving suggestions for future work.

Chapter 2: LITERATURE REVIEW

2.1 INTRODUCTION

The core aim of a DC-DC boost converter is to keep the output voltage at a fixed reference, no matter how the input source or the load changes [12]. Rapid return of voltage to its reference after a sudden load step is essential so that sensitive electronics remain protected. Any dip in voltage must be kept as small as possible. Low ripple in both the inductor current and the output voltage is desired to cut stress on magnetic and capacitive parts, which in turn raises efficiency and extends component life [13]. High conversion efficiency is also required so that less energy is lost as heat and a compact design may be used in space-limited applications [14]. To meet these goals, many researchers have explored various control techniques. Traditional PI controllers, sliding mode control, fuzzy logic systems, and artificial intelligence-based methods were all proposed in earlier studies [15-18]. This chapter will outline the previous studies that were carried out to secure stable voltage regulation through different methods.

2.2 PREVIOUS STUDIES

Step-up DC-DC boost converter was proposed by Adnan et al. [19] to improve voltage regulation and transient performance by the inclusion of a PID controller in the feedback loop. A simple PID controller was tuned by a trial-and-error method and inserted in the feedback loop of a conventional boost topology. With an input voltage varying between 90 V, 100V and 110 V, the converter output was held at 200 V with less than 3 % overshoot while compared to more than 50 % overshoot in the open-loop case. Key parameters such as a 400 μH inductor, 100 μF output capacitor, 50 Ω resistive load, and controller gains (K_p =

0.0033, K_i = 6.43, Kd = 0.0027) were used to demonstrate stable performance under load and source changes. By reducing overshoot and eliminating steady-state error, the proposed scheme was shown to give much better voltage regulation and dynamic response. Figure 2.1 shows their proposed PI controller-based Boost converter system.

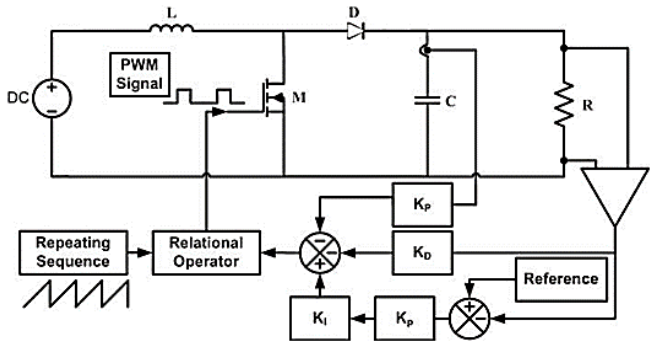


Figure 2.1: Proposed PI controller-based DC-DC Boost converter by Adnan et al. [19].

Over time, a variety of schemes have been developed to both stabilize the system and accelerate its transient behavior. Among these are fuzzy-logic–based regulators [20], neural-network controllers, and classic PID and PI designs [21] [22]. Namon Kunjittipong and Sudarat Khwan [23] proposed a PI controller for a boost-derived hybrid converter (BDHC) to supply both DC and AC loads. The controller parameters were first calculated from the mathematical model of a single-stage boost converter and then tuned for the hybrid setup. A dual-loop

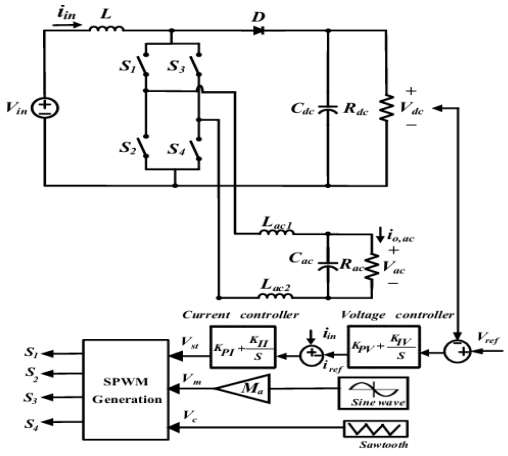


Figure 2.2: Proposed PI Controller structure [23].

Structure show in Figure 2.1 was employed with initial voltage-loop gains of K_{PV} = 0.03 and K_{IV} = 0.83, and current-loop gains of K_{PI} = 0.0293 and K_{II} = 2.7556. After tuning, the final gains were set to K_{PV} = 0.03, K_{IV} = 1.5, K_{PI} = 0.5, and K_{II} = 2. The BDHC was simulated under five scenarios including DC reference changes, input voltage swings, AC reference shifts, and variations in both DC and AC loads and was shown to maintain 100 V DC and 35.35 V_{rms} AC outputs with stable response in all cases. However, the study was limited to simulation only and real-world effects such as component tolerances, switching losses, and noise were not examined and also no experimental validation was provided.

In Shayeghi et al. [24] applied a cascade PD–PI controller to a boost converter and its gains were optimized by the Grey Wolf Optimization algorithm to tune its proportional, derivative, and integral gains based on the ISTAE performance index. The tuned parameters were found to be K_P = 10.4932, K_I = 28.0809, K_D = 26.9060, and K_{P2} = 23.4671. Four simulation cases were studied. In Case 1, the PD–PI scheme reduced overshoot error: the ISTAE fell from 331.5 (PID) to 311.3, the ITAE from 324.2 to 313.1, and the IAE from 335.8 to 314.2. Undershoot error metrics were reported as ISTAE = 198 versus 130, ITAE = 197.6 versus 128.7, and IAE = 196.8 versus 126.4 for PD–PI and PID, respectively. However, the settling time was reduced from 0.0153 s (PID) to 0.0051 s. Under these conditions, the PD–PI scheme achieved an ISTAE of 311.3 compared to 331.5 for a standard PID controller which representing about a 6 % improvement in the performance index.

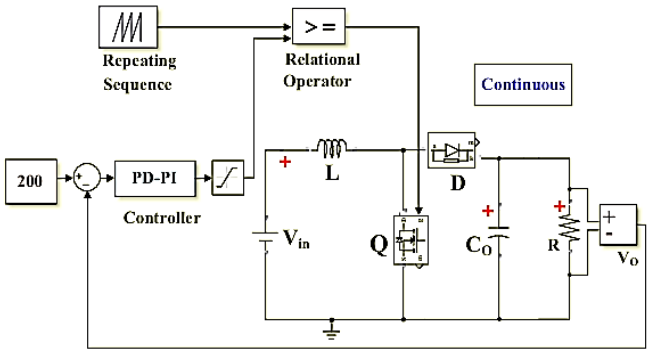


Figure 2.3: Simulation model proposed by [24].

F. Punnya Priya and K. Latha [25], an input-output feedback linearization controller was applied to a 600 W boost converter (Vin = 30 V, V_{oref} = 72 V, RL = 9.426 Ω, L = 100 mH, C = 110 μF, f_s = 50 kHz) and simulated in MATLAB/Simulink shown in Figure 2.4. The feedback coefficients were set using $\omega_n = 3.97\times10^3$ rad/s and $\zeta = 0.114$. Four test scenarios were studied: at start-up the settling time was cut from 0.22 s (PI) to 6 ms with 2.05 % overshoot and when V_{in} was stepped from 50 V to 30 V the response time fell from 1.3 s to 5 ms with 0.694 % overshoot. Under a load change 9.426 Ω to 17.24 Ω, the settling time dropped from 0.9 s to 5 ms with 12.5 % overshoot and for a reference step 55 V to 72 V the settling time improved from 0.15 s to 5.5 ms with 1.388 % overshoot. These results demonstrated greatly accelerated dynamic response and tighter voltage regulation.

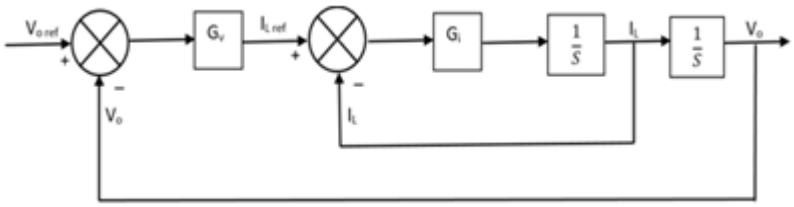


Figure 2.4: Block diagram of the designed model by [25].

In Sasikala and Kumar [26], a PI controller was applied to a boost DC–DC converter designed and was tuned by the Ziegler-Nichols method to set its proportional and integral gains. The converter circuit include an IGBT switch, inductor, diode, output capacitor, and resistive load which was modeled in

MATLAB/Simulink with a PWM generator was used to convert the PI output into switching pulses shown in Figure 2.5. Simulation results showed that the

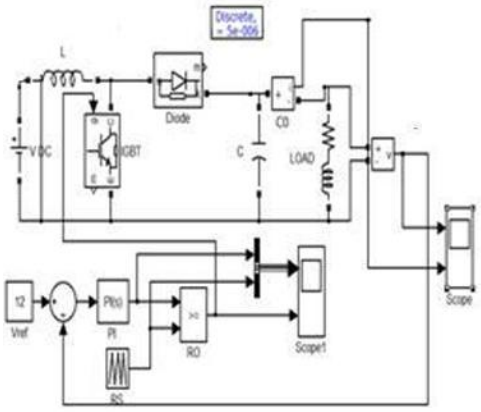


Figure 2.5: Simulation of the PI controller boost converter by [26].

output voltage was held steadily at its reference level under normal conditions which demonstrated effective voltage regulation. However, no quantitative performance data such as overshoot, settling time, or ripple were reported and the study was limited to simulation only. Sachin and Gurunayk Nayak [27] designed a PWM-based sliding mode controller for a DC–DC boost converter and was compared with a PI controller in MATLAB/Simulink. The converter was specified with a 12 V input, a 2.5 mH inductor, a 20 μF output capacitor, a 60 Ω load (varied up to 1100 Ω), and a 20kHz switching frequency to produce 24 V at the output. The sliding mode scheme was to hold the output at 24 V with a settling time of 12 ms and a steady-state error of 0.56 V whereas the PI controller yielded a settling time of 15 ms and an error of 1.07 V. The output ripple was kept below 1 % in steady state. Load changes were applied and the sliding mode approach was found to be robust which try to maintain consistent performance across all conditions. However, only simulation studies were conducted and no practical factors such as component tolerances, switching losses, and measurement noise were examined.

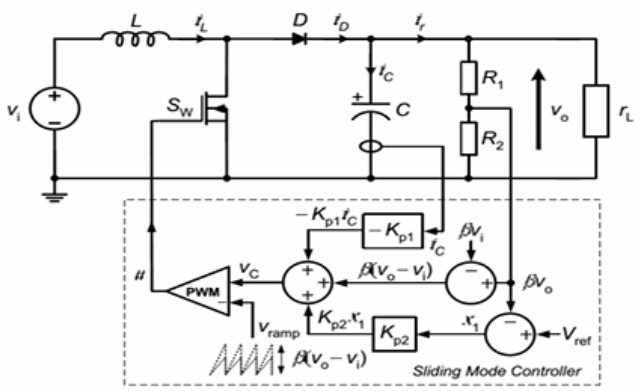


Figure 2.6: Sliding mode structure designed by [27].

Shadoul et al. [28] presented analysis and simulation of a DC-DC boost converter for PV applications. First, the converter was represented by a transfer function that related duty ratio to output voltage. A PI controller was designed by use of the root-locus method on the linear model. The proportional gain was chosen as $K_p = 1.2539 \times 10^{-4}$ and the integral gain as $K_i = 0.0251$. Zeros and poles were placed in the s-plane to achieve a stable closed-loop response. The controller and the nonlinear converter model were implemented in MATLAB/Simulink. Closed-loop performance was tested under source and load disturbances. Results showed that without a controller, the loop was unstable. A proportional term was added, and stability was achieved but a steady-state error was present. After a zero and a pole were added via the PI controller, the response was stable and accurate. A step response test with a 40 V input change was performed and the output voltage was returned to the reference in 0.1 s with no overshoot.

A dual-loop control method based on a PI topology was proposed by Kifayat et al. [29] for a DC-DC boost converter to step up a 24 V input to 36-48 V. Inner and outer loops were defined to regulate inductor current and output voltage, respectively. Mathematical equations for the boost converter were derived and two PI controllers were tuned ($K_p = 0.4$, $K_i = 80$ for both loops). The complete control scheme was implemented in MATLAB/Simulink shown in Figure 2.7.

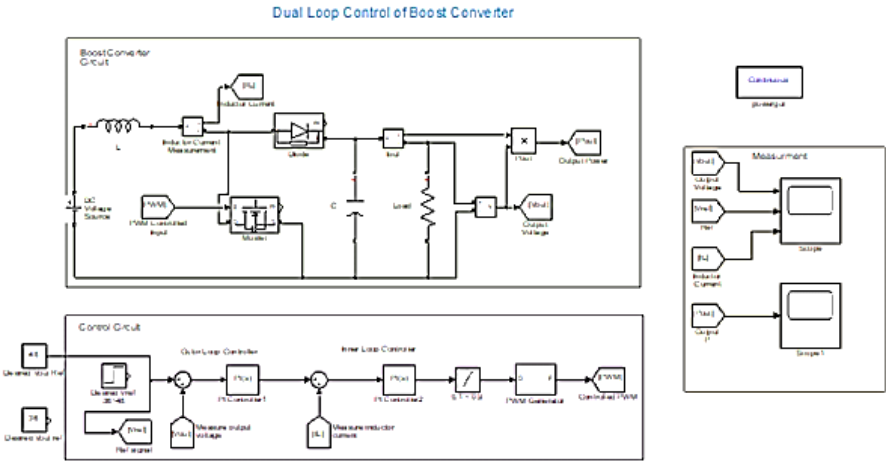


Figure 2.7: Dual loop control of Boost converter design [29].

Three scenarios were simulated: fixed output voltage, step change from 36 to 48 V, and sudden connection of a 1 kW load at 0.1 s. Under a fixed 36 V reference, a steady output with 95 % efficiency was recorded. During the step change, voltage dips were reduced to negligible levels and inductor ripples stayed below 0.3 A. The results showed that in the sudden-load case, the output voltage returned to the reference by 0.5 s with negligible dip and an efficiency of about 98 %. Variable output was achieved by adjusting the switch delay angle.

Performance of fuzzy and PI controllers was evaluated by Lenine et al. [30] for a boost converter with active power-factor correction. Two control objectives voltage regulation and sinusoidal input current were defined. A boost converter was modelled with inner current and outer voltage loops. Fuzzy logic rules were formulated using seven linguistic sets, Mamdani inference, and bisector defuzzification. A conventional PI regulator was implemented in parallel for comparison. The control scheme was in MATLAB/Simulink with a 400 V DC

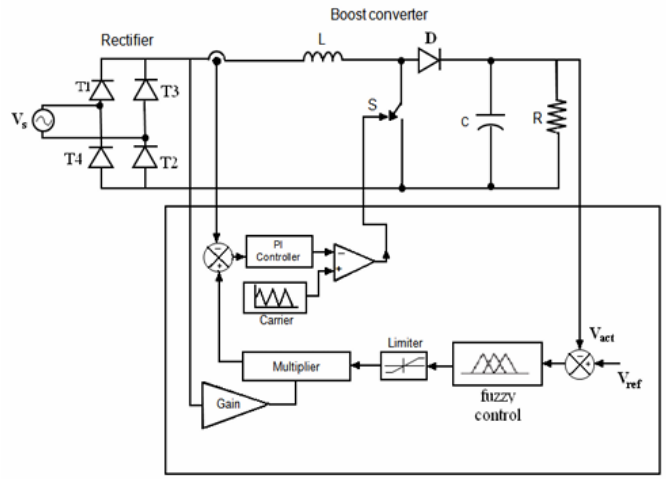


Figure 2.8: Proposed system designed by Lenine et al. [30].

reference and a full-bridge AC-DC front end. Three conditions open-loop, PI-controlled, and fuzzy-controlled were simulated at a 90 V line voltage. Input current, output voltage, and total harmonic distortion (THD) were recorded. Fuzzy control was shown to raise power factor to 0.999 and reduce THD to 3.9 %. Settling time was shortened from 0.22 ms under PI control to 0.065 ms under fuzzy control.

Rabiaa et al. [31] presented case cade control converter with a PI controller. An averaged model of a DC–DC boost converter in continuous-conduction mode was derived, and a cascade control structure was adopted with an inner current loop and an outer voltage loop. Conventional PI controllers tracked the reference current and eliminated load disturbances. The mathematical model and controllers were implemented in MATLAB/Simulink

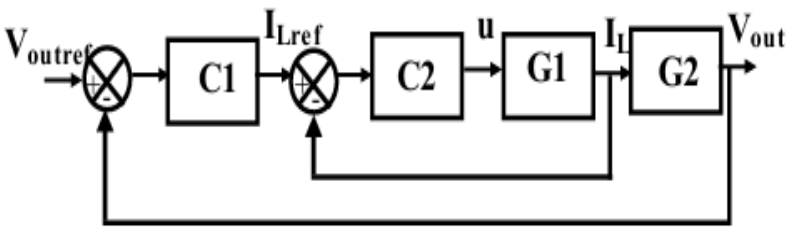


Figure 2.9: Controller block diagram [31].

and simulations were carried out under variable input voltage and load resistance conditions. In this work, a continuous-conduction-mode boost

converter was first represented by an averaged state-space model obtained by combining the on- and off-state equations around a nominal operating point. A two-loop cascade control structure was then adopted: an inner current loop was used to force the inductor current to follow a reference, and an outer voltage loop was employed to regulate the output voltage. Both loops were closed by conventional PI controllers, and their gains were selected to shape rise time, overshoot, and steady-state error Simulation results indicated that, The control scheme was implemented in MATLAB/Simulink using a boost stage with an input of 186 V, a 39 mH inductor, a 700 μF filter capacitor, a 53 Ω load, a loop coefficient α = 0.6, a reference current of 21.5 A, and a desired output of 466 V. Under an input step from 186 V down to 160 V at t = 0.6 s and back at t = 1.2 s, the output was returned to its set point in 0.2 s but a 13.73 % overshoot was observed. When the load was varied from 54 Ω to 64 Ω and then to 50 Ω at the same instants the voltage disturbance was rejected rapidly, and the inductor current tracked its reference smoothly. The cascade loop achieved improved rise time, disturbance rejection, and steady-state accuracy compared to single-loop control. However, all evaluations were limited to simulation, and optimal performance was shown only near the nominal operating point due to converter nonlinearity. Validation on hardware and exploration of alternative control methods for wider operating ranges were suggested.

Three-port high-gain boost converter was proposed by Yuvaraj et al. [32] that uses two switching cells connected to separate input ports and a single magnetizing inductance as a common energy paths. A small-signal model was

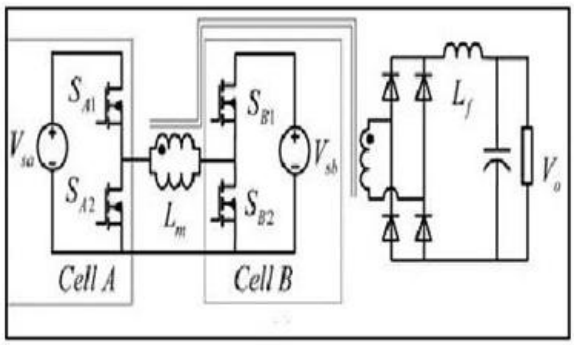


Figure 2.10: Three port converter system [32].

derived for each operation mode (dual-output, dual-input, and single-input) and a decoupling network was introduced to allow independent current and voltage loops. A novel PWM scheme with three control voltages (Vc1, Vc2, Vc3) was employed to perform maximum power point tracking on the PV port while regulating battery and load voltages. The system was implemented in MATLAB/Simulink using MOSFET switches, coupled inductors, and RLC filters. Simulation results showed that high voltage gain was achieved with only four power switches with that switch stress was reduced, and that inductor currents maintained proper ripple characteristics as shown in the waveforms. Converter efficiency remained high over a wide input range.

A non-ideal differential boost inverter (DBI) with cascaded PI control was presented by Arunkumar et al. [33]. A fourth-order averaged small-signal model was derived, and root-locus methods were used to establish initial PI gain bounds. Optimization via genetic algorithm (GA) and bacterial foraging optimization algorithm (BFOA) was then applied to refine the controller parameters for rapid transient response and low steady-state error. he PI controller parameters were first tuned via a genetic algorithm (GA) with a population of 75, binary-coded chromosomes, ten multi-point crossover iterations, kP bounds [1×10^{-6}, 1×10^{-4}], and k_I bounds [1×10^{-7}, 1×10^{-5}]. The GA minimized rise time (tr), settling time (ts), peak overshoot (P_0), and steady-state error (ESS) and yielded kP = 3×10^{-5} and kI = 8×10^{-6} for stable output under line

and load transients. A bacterial foraging optimization algorithm (BFOA) was then applied, using ten bacteria, ten iterations, chemotactic size = 4, reproductive loops = 4, elimination-dispersal loops = 2, swim length = 4, and dispersal probability = 0.2. This led to further reduction in computational effort while preserving stability. A BFOA implementation, following elimination-dispersal and chemotaxis strategies, was also carried out to further improve

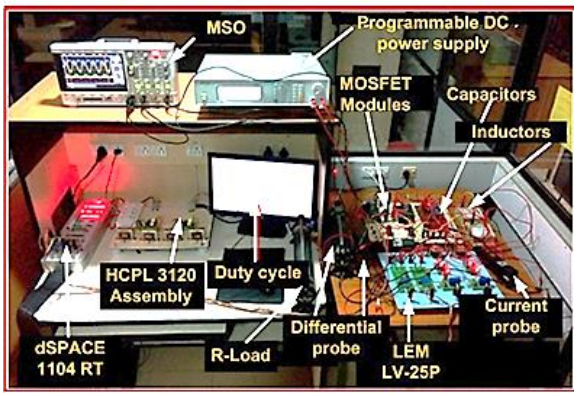


Figure 2.11: Hardware setup of the proposed system [33].

Performance under line and load disturbances. Real-time validation was performed on a dSPACE 1104 platform with a 1 μs sampling time, using both resistive and motor loads. A comparative assessment demonstrated that both GA and BFOA-tuned PI controllers achieved settling times of 20 ms under line disturbances, overshoots below one cycle, and THD <5%, outperforming the traditional PI design. All results were supported by hardware tests showing in Figure 2.11 and results demonstrated stable performance across different voltage levels and load types. However, extension to three-phase systems, robustness studies under temperature and component tolerances, and broader environmental testing were recommended for future work.

2.3 SUMMARY AND IMPLICATIONS

This chapter reviewed several research works on DC-DC boost converters with special attention to how different control methods affect system performance. Among all techniques studied, the PI controller was one of the most

widely used due to its simple design and ability to control output voltage effectively. However, the review showed that the PI controller does not always guarantee the best performance unless its parameters are selected and tuned properly. When the proportional and integral gains are chosen carefully, the PI controller can reduce overshoot, shorten settling time, and minimize steady-state error. Many studies confirmed that a properly tuned PI controller helps the boost converter maintain a stable output voltage even under sudden changes in input voltage or load. In some cases, researchers used trial-and-error, mathematical modeling, or intelligent algorithms like Genetic Algorithm (GA) and Bacterial Foraging (BFOA) to tune the PI parameters. These tuning methods made the system more reliable and faster in response. From this review, it is clear that the PI controller can provide high performance in boost converter systems when it is tuned correctly. This finding supports to design and implement a boost converter using a well-tuned PI controller to achieve stable voltage output, high efficiency, and fast dynamic response.

.

Chapter 3: METHODOLOGY

3.1 OVERVIEW OF THE RESEARCH APPROACH

A simulation-based method was used in this study to design a DC-DC boost converter controlled by a PI controller. The overall methodology was implemented using MATLAB Simulink. The design process was divided into several steps to ensure that the converter could operate efficiently and maintain a stable output voltage under varying conditions. The process began by selecting the key parameters for the boost converter including the input voltage, desired output voltage, power, acceptable ripple etc. These values were used to define the operating range and design targets of the system. Based on the chosen parameters, the converter was mathematically modelled by analysing its switching behaviour. Once the mathematical model was developed, then the main circuit parameters were calculated. These included the values of the inductor, capacitor, load resistance, voltage ripple, and duty cycle. The calculations were performed to ensure smooth output voltage with minimal ripple and proper current control. After the design parameters were finalized, a Simulink model of the boost converter was created in MATLAB/SIMULINK. A PI controller was then designed to regulate the output voltage. Once the controller was added, the system was tested through simulation. If the PI controller did not produce a stable and accurate output, the gain values were adjusted and the process was repeated. The controller was tuned properly so that it always provides the consistent desired output voltage. After achieving a properly tuned response, simulation results such as output voltage and current were recorded. The performance of the system was evaluated using standard error metrics which helped to assess how well the converter performed under the given conditions. A summary of the full design process is shown in Figure 3.1,

which outlines the steps from parameter selection to controller tuning and final evaluation.

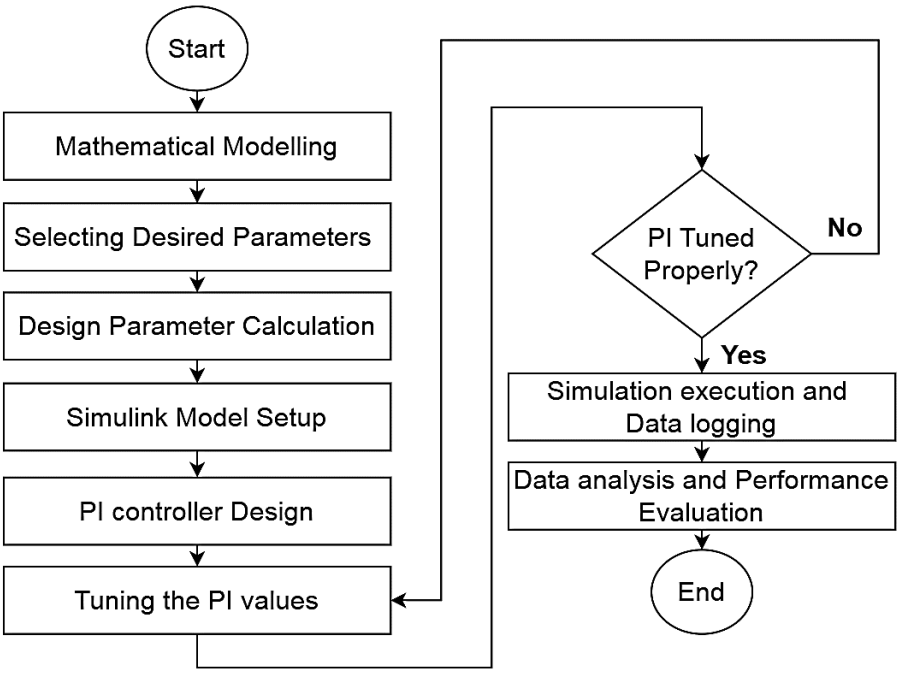


Figure 3.1: Flowchart of the overall workflow.

3.2 MATHEMATICAL MODELLING OF THE BOOST CONVERTER

A boost converter is a type of DC–DC converter that raises a lower input voltage to a higher output voltage level. It stores energy in an inductor during one part of the switching cycle and transferred that energy to the load during the other part. The circuit typically consists of an inductor (L), a controlled switch, a diode (D), a capacitor (C), and a load resistor (R). The converter operates in two main modes: when the switch is ON which stated as conducting and when the switch is OFF which is stated as non-conducting [34]. The Figure 3.2 shows the prototype design of the typical boost converter consisting all of the equipment. It includes an input voltage source Vin, an inductor L, a power switch Q which is a MOSFET, a diode D, an output capacitor Co, and a resistive load R. The voltage across the output is denoted as Vo, and the current flowing through the inductor is represented by i_L. The diode current is marked as i_D, the output current as i_o,

the capacitor current as i_C, and the switch current as i_S. The directions of currents and polarities of voltages are indicated in the figure to clearly define the behaviour of the components. The boost converter operates by rapidly switching the MOSFET ON and OFF with transferring energy from the input to the output while boosting the voltage level. The switch controls the power flow from the source to the load by alternating between ON and OFF states at high frequency using a PWM signal [34]. The capacitor acts as a voltage buffer and provides current to the load when the switch is ON. The operating principle of the boost converter in Continuous Conduction Mode (CCM) can be described using two main operating intervals: Mode I (switch ON) and Mode II (switch OFF). This switching operation is the basis of the converter's functionality.

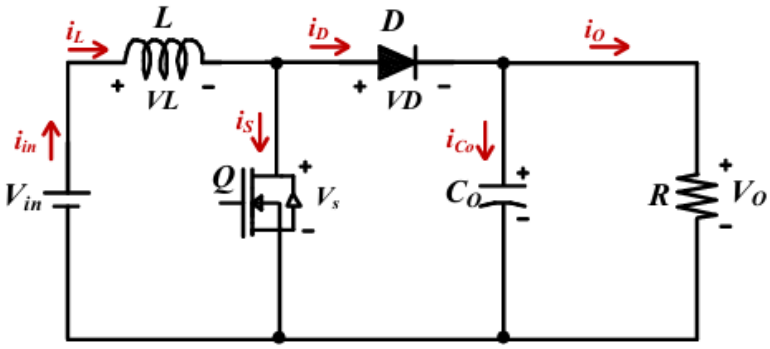


Figure 3.2: Typical Boost converter circuit [24].

During Mode I, the switch Q is turned ON, and the diode D becomes reverse-biased. As shown in Figure 3.3, the current from the input source Vin flows through the inductor L and the closed switch to ground. This forms a loop, and the inductor begins to store energy in the form of a magnetic field [35]. The current through the inductor increases linearly. By applying Kirchhoff's Voltage Law (KVL) across the inductor, the voltage across it can be written as:

$$V_L = V_{in} \tag{3.1}$$

Using the inductor's voltage-current relationship:

$$\frac{di_L}{dt} = \frac{V_{in}}{L} \tag{3.2}$$

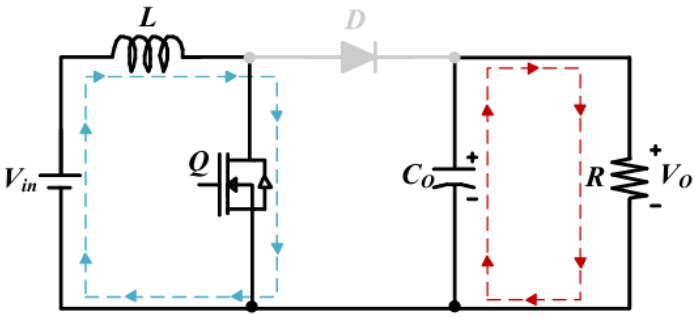


Figure 3.3: Operation of the converter when in Mode I [24].

Since the diode is OFF, no energy is delivered from the inductor to the output at this time. The output capacitor Co supplies the load current during this period shown in clearly in the Figure 3.3 and as a result it starts to discharge slightly. The output voltage decreases gradually depending on the load. The change in output voltage is expressed as:

$$\frac{d_{v_{out}}}{dt} = -\frac{V_{out}}{RC} \tag{3.3}$$

The key effect of the inductor in this mode is energy accumulation, while the capacitor supports the load.

In Mode I, the switch Q is turned OFF, as shown in Figure 3.4. The inductor current cannot drop suddenly and continues to flow due to the energy

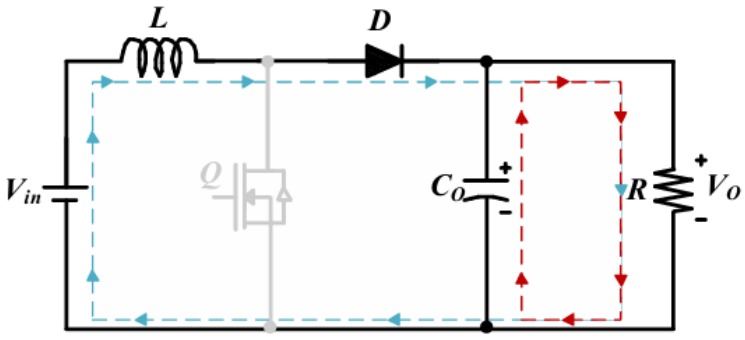


Figure 3.4: Operation of the converter when in Mode II [24].

stored in the magnetic field. This energy is now redirected through the forward-biased diode D and delivered to both the output capacitor and the load. The inductor current decreases during this time. By applying Kirchhoff's Voltage Law across the loop including Vin, L, D, and the output we get:

$$V_L = V_{in} - V_{out} \tag{3.4}$$

$$\frac{d_{i_L}}{dt} = \frac{V_{in} - V_{out}}{L} \tag{3.5}$$

In this state, the capacitor Co is charged by the inductor, and at the same time, it supplies the load. The rate of change of output voltage is determined by:

$$\frac{d_{v_{out}}}{dt} = -\frac{i_L - \frac{V_{out}}{R}}{C} \tag{3.6}$$

During this interval, the inductor releases its stored energy, and the output capacitor is both charged and used to meet the load demand. To represent the dynamic behavior of the boost converter over one complete switching cycle, it is necessary to consider both operating intervals: when the switch is ON and when it is OFF. Since the converter transitions between these two states during every switching cycle, the net effect on the inductor current can be captured by averaging the behavior across both states, weighted by the time fraction each state occupies. By applying state-space averaging, the total rate of change of the inductor current over the full switching cycle is expressed as the weighted sum of the two intervals. Therefore, the equation becomes [34]:

$$\frac{d_{i_L}}{dt} = d \times \frac{V_{in}}{L} + (1 - d) \frac{V_{in} - V_{out}}{L} \tag{3.7}$$

This expression (3.7) reflects the combined effect of both energy accumulation and release phases of the inductor. The first term represents the inductor charging during the ON state, and the second term represents discharging during the OFF state. These equations represent the state-space averaged model of the boost converter under continuous conduction. The model includes the effects of all key components and forms the foundation for control system design and performance analysis.

3.3 CALCULATION OF DESIGN PARAMETERS

The performance of a boost converter depends heavily on the correct selection of its electrical components. To achieve the desired output voltage with

minimal ripple and stable operation, the values of the inductor, capacitor, load resistance, and duty cycle must be carefully calculated. This section describes the design specifications used for the converter and explains how each parameter was derived.

3.3.1 DESIGN SPECIFICATION

The boost converter in this design is intended to step up a DC input voltage of 60 V to a regulated output voltage of 110 V. The maximum output power is specified as 400 W. A switching frequency of 20 kHz is selected to ensure fast operation while avoiding excessive switching losses. To maintain high quality and smooth output, the allowable ripple for both the inductor current and output voltage is chosen to be very low approximately 0.1% of their respective peak values. These ripple values help minimize output noise and stress on the components. Based on these conditions, the converter components must be sized accordingly to handle the voltage, current, and energy transfer.

3.3.2 PARAMETER CALCULATION

To design the boost converter accurately, a set of standard equations was used to calculate the values of essential components such as the inductor, capacitor, load resistance, and duty cycle. These calculations were based on the desired input and output conditions, the switching frequency, and the target ripple limits. Each parameter was carefully selected to ensure high efficiency, low noise, and stable output performance during operation. The first step in the design process was to determine the maximum output current. Since the power delivered to the load is 400 W and the output voltage is 110 V, the output current can be calculated using the basic power equation:

$$I_{out,max} = \frac{P}{V_{out}} \tag{3.8}$$

Substituting the known values:

$$I_{out,max} = \frac{400}{110} = 3.6364\ A$$

This value indicates the maximum current that the converter must supply to the load. The ripple in inductor current was limited to 0.1% of the output current for ensuring a smooth and continuous inductor waveform. A higher ripple could increase electromagnetic interference and stress the components, while a lower ripple improves system stability and reduces output noise. The inductor ripple current is further scaled by the output-to-input voltage ratio, and the equation is given as:

$$\Delta I_L = 0.001 I_{out,max} \frac{V_{out}}{V_{in}} \quad (3.9)$$

Substituting the values, it becomes $\Delta I_L = 0.001 \times 3.6364 \times \frac{110}{60} = 0.0067$ A. This small value helps reduce voltage ripple at the output and limits stress on the inductor and switch. Similarly, the ripple allowed in the output voltage was kept to only 0.1% of the total output voltage to ensure a very stable DC supply to the load. The ripple voltage is calculated as:

$$\Delta V_{out} = 0.001 \times V_{out} \quad (3.10)$$

It becomes, $\Delta V_{out} = 0.110$ V. The inductance value was calculated using the standard boost converter formula that relates input/output voltages, ripple current, and switching frequency:

$$L = \frac{V_{in}(V_{out} - V_{in})}{\Delta I_L\, f_s\, V_{out}} \quad (3.11)$$

This equation (3.11) ensures that the inductor can store and release the right amount of energy during each switching cycle without causing excessive ripple or saturation. Using the known values, the inductance comes out to approximately 0.2045 H. A higher inductance results in lower ripple, but it also increases the size and cost of the component. The capacitor is responsible for filtering the output voltage and supplying the load when the switch is ON. Its

value depends on the ripple current, voltage ripple, and switching frequency. The capacitance was calculated using:

$$C = \frac{I_{out,max}(1-\frac{V_{in}}{V_{out}})}{f_s \, \Delta V_{out}} \tag{3.12}$$

Substituting the known values, the result is approximately 751.31 μF. A larger capacitor reduces voltage ripple and improves stability but also increases physical size and cost. The load resistance was determined using Ohm's law, based on power and output voltage:

$$R = \frac{{V_{out}}^2}{P} \tag{3.13}$$

Finally, the duty cycle, which controls how long the switch remains ON during each cycle, was calculated. A higher duty cycle means more energy is stored in the inductor, while a lower duty cycle means more time is allowed for energy transfer to the output. The equation is:

$$d = \frac{V_{out}-V_{in}}{V_{out}} = 0.4545 \tag{3.14}$$

This means that the switch stays ON for approximately 45.45% of each switching period and off for the remaining. Table 3.1 summarizes the complete set of design specifications along with the final values of the calculated parameters used for the boost converter. These calculated parameters serve as the foundation for building and simulating the converter. Each component was chosen to balance performance, size, and efficiency, and to ensure that the converter can operate reliably with low ripple and stable output voltage under the given load conditions.

Table 3.1: Design specification and final Calculated Parameters for the Boost Converter.

Parameter	Value	Units
Output Power, P	400	W
Input Voltage, Vin	60	V
Output Voltage, V_{out}	110	V
Switching Frequency, fs	20000	Hz
Output Current, $I_{out,max}$	3.6364	A
Inductor Ripple, ΔI_L	0.0067	A
Voltage Ripple, ΔV_{out}	0.110	V
Inductance, L	0.2045	H
Capacitance, C	751.31	μF
Load Resistance, R	30.25	Ω
Duty Cycle, d	0.4545	—

3.4 PI CONTROLLER DESIGN AND TUNING

For regulating the output voltage of the boost converter efficiently and accurately, a PI controller was designed and applied in a closed-loop control configuration. The purpose of this controller is to minimize the difference between the desired reference voltage and the actual output voltage of the converter with adjusting the control signal. Figure 3.5 illustrates the overall closed-loop structure of the converter system where the PI controller has been implemented. The reference signal denoted as R(s) represents the specified output voltage level which set as 110V. This signal is evaluated to the actual output voltage of the boost converter and the resulting difference is known as the error signal E(s). This is then processed by the PI controller. The PI controller consists of two main components: a proportional gain Kp and an integral gain Ki . The proportional part of the controller produces an output that is directly proportional to the present value of the error signal. This provides a fast reaction to changes and helps reduce the rise time of the response. However, a proportional controller alone cannot eliminate steady-state error completely.

Therefore, the integral component is used in parallel, which accumulates the error over time and adjusts the control signal to eliminate this error. This integration action is mathematically represented by 1/s in the Laplace domain which ensure that even small persistent errors are corrected over time. The combined output of the proportional and integral

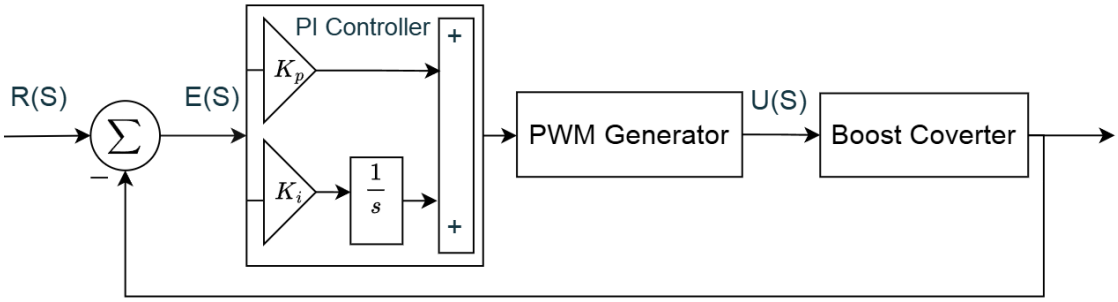


Figure 3.5: The converter's control system structured with PI controller in a closed-loop configuration.

paths is then summed and sent to the PWM generator. This PWM block translates the continuous control signal into a digital switching signal that can be sent to the gate of the switching element within the boost converter. By adjusting the duty cycle of the PWM signal, the energy transferred to the output is regulated, thus maintaining the desired voltage level. The boost converter receives the PWM signal as its control input, U(s) and uses it to regulate the power conversion process. The mathematical expression of the PI controller in the Laplace domain is given as:

$$\text{PI} = \left(K_p + \frac{K_i}{s}\right) \tag{3.15}$$

The output voltage of the converter is continuously monitored and fed back to the summation point to complete the loop. This feedback mechanism allows the controller to react to any disturbances or changes in load conditions promptly and thereby improving stability and dynamic performance. To ensure the PI controller performed effectively in regulating the output voltage of the boost converter, a tuning process was carried out using transfer function-based tuning

in Simulink. This method allows for automatic estimation and tuning of the controller parameters by analyzing the behavior of the boost converter model. The process began by configuring the PI Controller block in the Simulink model. Instead of manually guessing the proportional and integral gain values, the ``Tune'' button within the PI controller block was selected shown in Figure 3.6. This opened the Control System Tuner interface provided

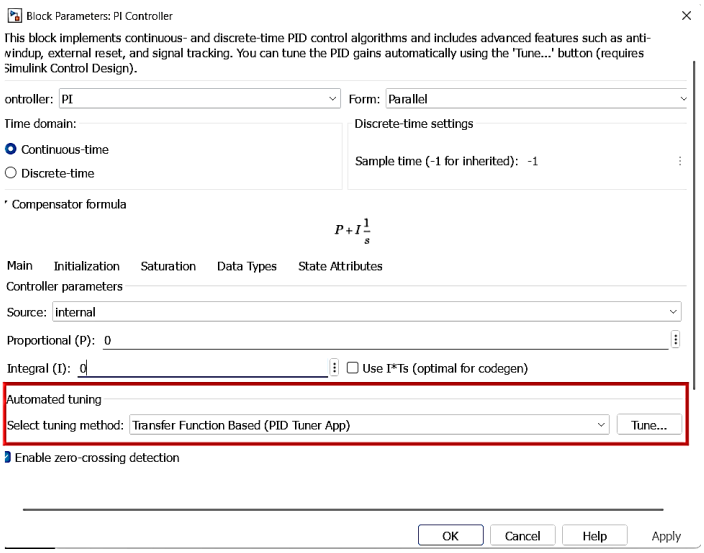


Figure 3.6: PI Tuner using the Transfer Function Based automated tuning.

by Simulink. In order to tune the controller, it was first necessary to define the plant model, which represents how the system responds to control inputs. Since the boost converter is a nonlinear, time-varying system, direct analytical modeling may be complex. Therefore, the "Create New Plant" option was chosen. This allowed Simulink to generate a plant model automatically using system identification. At this step, a step input signal was applied to the system, and the corresponding output voltage response was collected through simulation. This input-output pair was then used by Simulink to build a linearized approximation of the plant transfer function. Once the plant was created, the next step was to configure the desired response characteristics. In this, an underdamped response was selected. This type of response is generally preferred in power electronics because it allows for a faster settling time and

better tracking performance, while still keeping the overshoot within acceptable limits. After choosing the underdamped setting, the "Auto Estimate" option was enabled. This step allowed Simulink to automatically calculate optimal values for the proportional gain Kp and integral gain Ki, based on the plant dynamics and desired transient characteristics. Simulink provided a graphical tuning interface where the response curve could be adjusted in real-time by changing the sliders for response time and transient behavior. The tuning tool then automatically updated the Kp and Ki values to match the desired response. After completing the tuning, the updated PI parameters were applied directly to the controller block in the Simulink model. A test simulation was then run to observe the system behavior using the tuned values.

3.5 SIMULATION ENVIRONMENT AND MODEL SETUP

In this study, the entire design, analysis, and control of the DC-DC boost converter were carried out using MATLAB Simulink which is a widely used simulation platform developed by MathWorks. Simulink was chosen as the simulation environment because of its graphical, block-based interface, which allows engineers to model, simulate, and analyze dynamic systems without writing lengthy code. It provides an intuitive way to connect system components which makes it ideal for power electronics and control system modeling. One of the key advantages of Simulink is its real-time simulation capability which helps in visualizing system behavior step by step. It also supports customizable blocks, built-in solvers, and control system tuning tools, which made it especially useful for designing and optimizing the PI controller used in this boost converter. The Simulink model shown in Figure 3.7 represents the complete structure of the DC–DC boost converter, integrated with a PI controller in a closed-loop system.

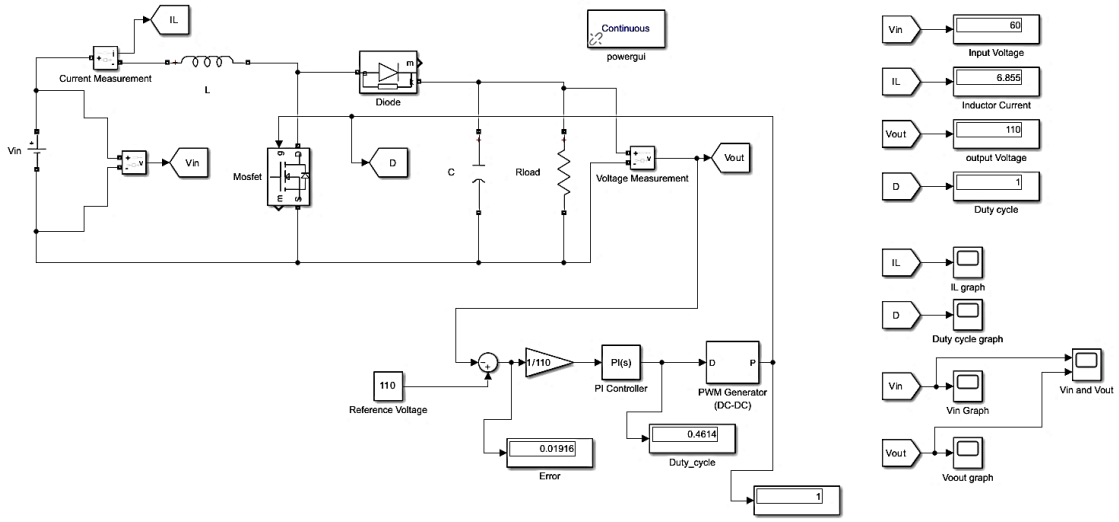


Figure 3.7: Boost converter with PI controller SIMULINK model.

3.6 DEFINITION OF PERFORMANCE METRICS

To evaluate how well the designed boost converter performs under closed-loop control using the PI controller, a set of time-domain and error-based performance metrics were used. These metrics help understand how accurately and quickly the system responds to changes, as well as how close the output stays to the desired reference.

3.6.1 Time-Domain Performance Metrics

The following key performance parameters were measured from the system's step response:

1. **Rise Time**: This is the time required for the output to go from 10% to 90% of its final steady-state value.
2. **Settling Time**: The time it takes for the output to stay within a small percentage (usually ±2% or ±5%) of the final value without oscillation.
3. **Overshoot**: This is how much the output exceeds the reference value, expressed as a percentage.
4. **Gain Margin and Phase Margin**: These represent the stability of the system.

These time-domain metrics are essential in confirming that the PI controller provides a fast, smooth, and stable response in the boost converter system.

3.6.2 Error-Based Performance Metrics

To further analyze the system's tracking performance over time, the following integral error metrics were used:

1. **IAE (Integral of Absolute Error)**:

$$\text{IAE} = \int_0^T |e(t)|\, dt \tag{3.16}$$

It sums the total absolute error over time. Lower IAE values indicate better tracking performance.

2. **ISE (Integral of Squared Error)**:

$$\text{ISE} = \int_0^T e(t)^2 dt \tag{3.17}$$

This penalizes large errors more than small ones by squaring the error. It's useful for measuring how severe the deviations from the reference are.

3. **ITAE (Integral of Time-weighted Absolute Error)**:

$$\text{ITAE} = \int_0^T t \times |e(t)|\, dt \tag{3.18}$$

This metric places more weight on errors that occur later in the response. A lower ITAE indicates faster settling and better long-term accuracy.

4. **MAE (Mean Absolute Error)**:

$$\text{MAE} = \frac{1}{N} \sum_{i=1}^{N} |y(t_i) - r(t_i)| \tag{3.19}$$

This is the average of the absolute error values.

5. **MSE (Mean Squared Error)**:

$$\text{MSE} = \frac{1}{N} \sum_{i=1}^{N} (y(t_i) - r(t_i))^2 \tag{3.20}$$

Like ISE, it emphasizes large errors but averaged over time. Both MAE and MSE should be as low as possible. A lower MAE means the output is consistently close

to the reference signal, while a lower MSE indicates fewer large deviations from the desired value. High values suggest poor tracking performance and larger errors. All of these metrics were calculated based on the simulation data from the MATLAB Simulink environment. These help in quantitatively comparing the accuracy and smoothness of the converter's response under PI control.

3.7 SIMULATION EXECUTION AND DATA ACQUISITION

After setting up the complete Simulink model of the boost converter with the PI controller, the simulation was executed for a total time duration of 5 seconds. This duration was chosen to ensure that both the transient and steady-state behaviors of the converter could be observed clearly. During the simulation, the system response to the reference voltage was monitored continuously to evaluate how effectively the PI controller maintained regulation. The data from the simulation was collected using the built-in Scope blocks available in the Simulink environment. These scopes were used to monitor and visualize key electrical signals such as the input voltage, output voltage, inductor current, and the duty cycle. Each scope was configured to log data during the simulation runtime. To analyze the system performance more precisely, the logged data was exported directly from Simulink to an Excel file using the data logging and exporting features. This allowed easy post-processing and evaluation of the control accuracy and dynamic response. From the exported data, performance metrics such as IAE, ISE, ITAE, MAE, and MSE were calculated by comparing the actual output with the reference voltage over time.

Chapter 4: RESULTS ANALYSIS AND DISCUSSION

4.1 PI CONTROLLER TUNING RESULTS

In this simulation, the controller is tuned using the auto-tuning feature in Simulink's PI Controller block. Summary of the PI Tuning Results have been shown in Table 4.1.

Table 4.1: Summary of The PI Tuning Results.

Parameter	Value	Unit / Description
Proportional Gain (K_p)	0.023954	—
Integral Gain (K_i)	8.2609	—
Rise Time	0.0459	seconds
Settling Time	0.0746	seconds
Overshoot	0.361	%
Peak	1	Normalized (unitless)
Gain Margin	26.3	dB (at 212 rad/s)
Phase Margin	70.2	degrees (at 30.3 rad/s)
Closed-Loop Stability	Stable	System remains stable under feedback

The tuning process have founded the best values for the Kp and Ki and this help the converter to respond quickly and accurately to any changes or disturbances. After tuning, the final values of the controller are found to be proportional Gain, Kp=0.023954 and integral Gain, Ki=8.2609. These parameters are put into the PI controller in the Simulink model to control the PWM signal. The proportional gain helps the controller react to the present error between the output voltage and the actual output. A small Kp like 0.023954 means the controller does not react too aggressively, which helps to avoid overshooting. The integral gain Ki=8.2609 removes any steady-state error over time. This value is high enough to

ensure that the converter eventually reaches the target voltage without drifting. The rise time was 0.0459 seconds. This means that the output voltage reaches 90% of the final value very quickly within just 45.9 milliseconds. The settling time is 0.0746 seconds, so the output voltage becomes stable within ±2% of the final value in 74.6 milliseconds. These are very fast times and show that the system responds quickly to the input. The overshoot is only 0.361%. This means that when the output voltage increases toward the reference value (110 V), it does not rise too much above the target. An overshoot below 1% is considered excellent in control systems, as it prevents stress on components and maintains safe operation. The peak value of the system response is 1, which is normal when normalized values are used. The gain margin is 26.3 decibels (dB) at 212 radians per second. Gain margin tells how much the gain can increase before the system becomes unstable. A high gain margin like this means the system is very stable. The phase margin is 70.2 degrees at 30.3 radians per second. Phase margin tells how much delay the system can handle before it becomes unstable. Again, a high value like this confirms that the converter is very robust and will not easily become unstable. Finally, the system is marked as "Stable" under closed-loop operation. This confirms that the controller will keep the system steady even when there are disturbances or changes in load.

4.2 SIMULATION OUTPUT

4.2.1 Output Voltage Waveforms (PI Tuned)

Figures 4.1 and 4.2 show the behaviour of both input and output voltages in the boost converter when the PI controller is used with the tuned gains (Kp=0.023954, Ki=8.2609). These waveforms are obtained through a 5-second simulation, and they clearly demonstrate how effectively the converter boosts the voltage and regulates it to the desired output level.

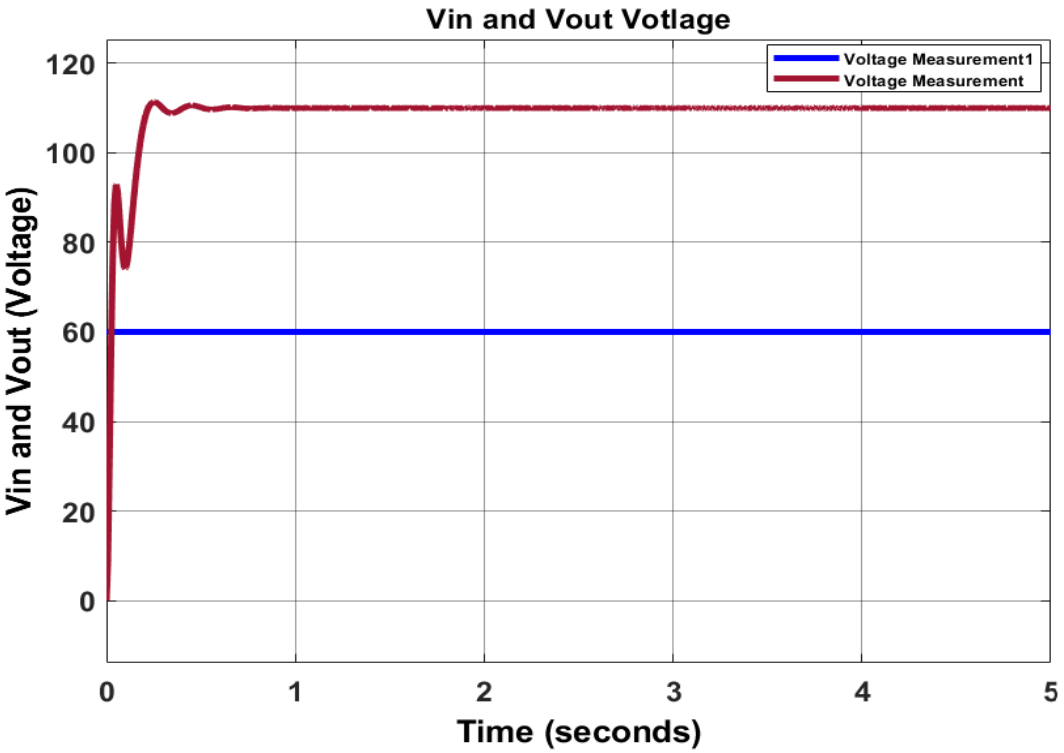


Figure 4.1: Input and output voltage graph from the Boost converter.

In Figure 4.1, the yellow horizontal line represents the constant input voltage (Vin) of 60 V. The blue waveform shows the output voltage (Vout), which starts from 0 V and begins to rise as soon as the converter is powered on. Within the first 0.5 seconds, the output voltage overshoots slightly, reaching a peak above 110 V, before settling down to a steady value. This behavior aligns with the previously measured rise time of 0.0459 s. In the waveform shown in Figure 4.1, the output voltage rises quickly and reaches around above 90 volts which is 90% of the target 110 volts within approximately 0.045 seconds. This matches the defined rise time and confirms that the system responds rapidly after startup. Similarly, the output voltage becomes steady and remains within ±0.1% of the final value. The voltage waveform quickly stabilizes after a very short period of fluctuation and maintains a nearly constant level around 110 V, as expected from a properly tuned PI-controlled boost converter. The minor oscillations during startup are due to the transient response of the system, which is normal for most power converters. However, the fast settling confirms that the controller

responds quickly and avoids long-term instability. This demonstrates good dynamic performance.

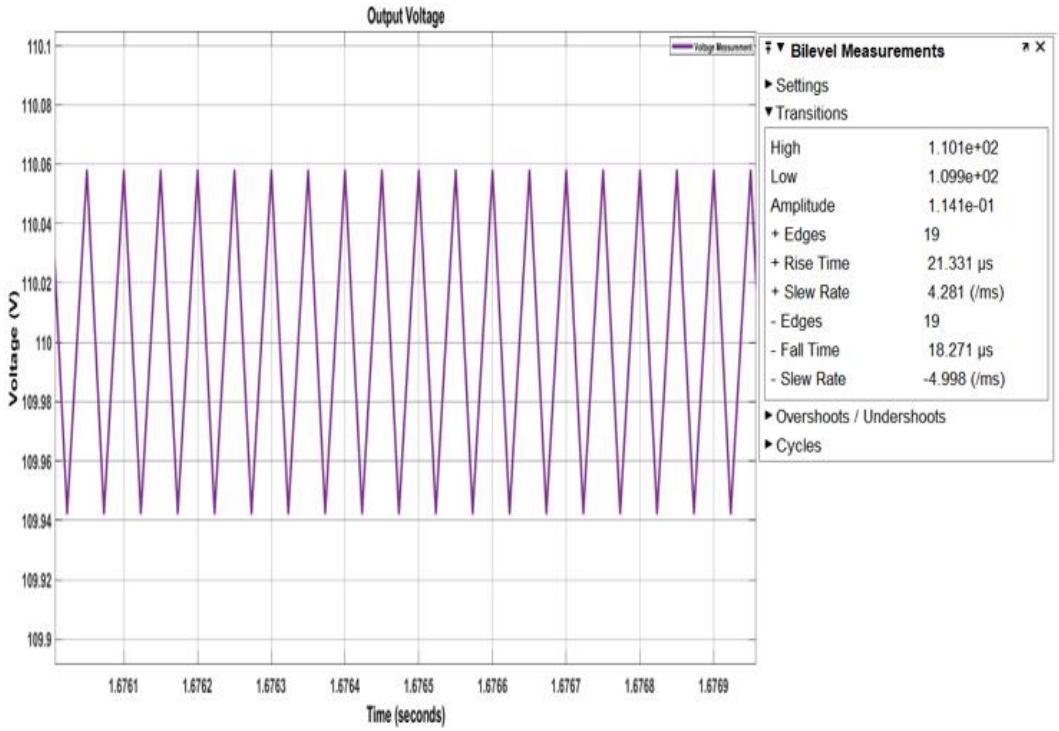


Figure 4.2: Output Graph signal statistics after settling the final value.

Figure 4.2 gives a closer look at the output voltage waveform after it has already settled. This zoomed-in view focuses on the output at around 3.006 seconds. The green line shows small repetitive fluctuations, which are normal ripples due to the switching nature of the converter. According to the signal statistics, the maximum voltage is 110.1 V and the minimum is 109.9 V. This gives a peak-to-peak ripple of 0.1153 V, or about ±0.0576 V around the mean. When this ripple is converted to percentage form, it is approximately 0.105%, which is very close to the design target of ≤ 0.1% ripple. This confirms that the inductor and capacitor values selected during the design phase are appropriate for reducing ripple.

4.2.2 Inductor Current Profiles

The performance of the inductor current plays a crucial role in determining whether the boost converter operates in Continuous Conduction Mode (CCM),

as designed. Figures 4.3 and 4.4 present the simulation results for the inductor current I_L over time. Figure 4.3 shows the full waveform of inductor current for the entire 5-second simulation, while Figure 4.4 provides a zoomed-in view with detailed signal statistics around time t=2.414 seconds, after the system has fully settled.

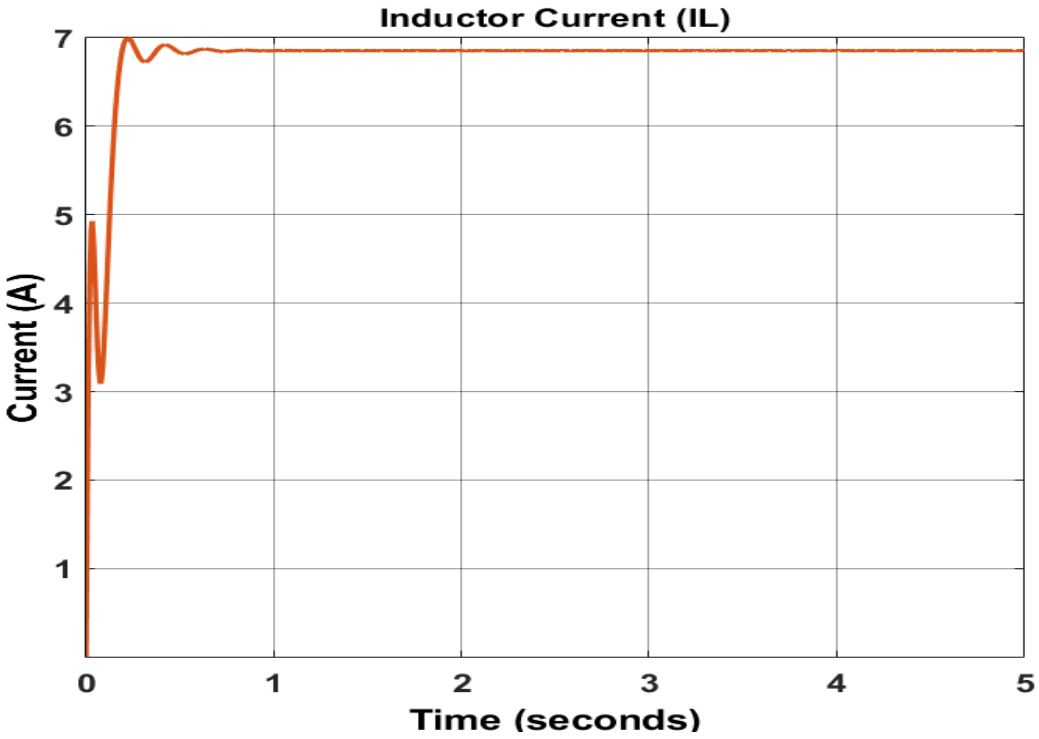


Figure 4.3: Inductor Current Graph.

In Figure 4.3, the inductor current starts from zero and rises quickly as the converter begins switching. Initially, during the first 0.5 seconds, the waveform exhibits noticeable oscillations due to the transient behavior of the system. The peak inductor current during this period briefly reaches slightly 7 A. These fluctuations are expected in the startup phase while the converter adjusts to the target voltage. After about 0.5 seconds, the current stabilizes and becomes nearly constant, indicating that the system has entered steady-state operation. The waveform flattens out around a current level of approximately 6.85 A, confirming that the system is operating in CCM, as the inductor current never drops to zero.

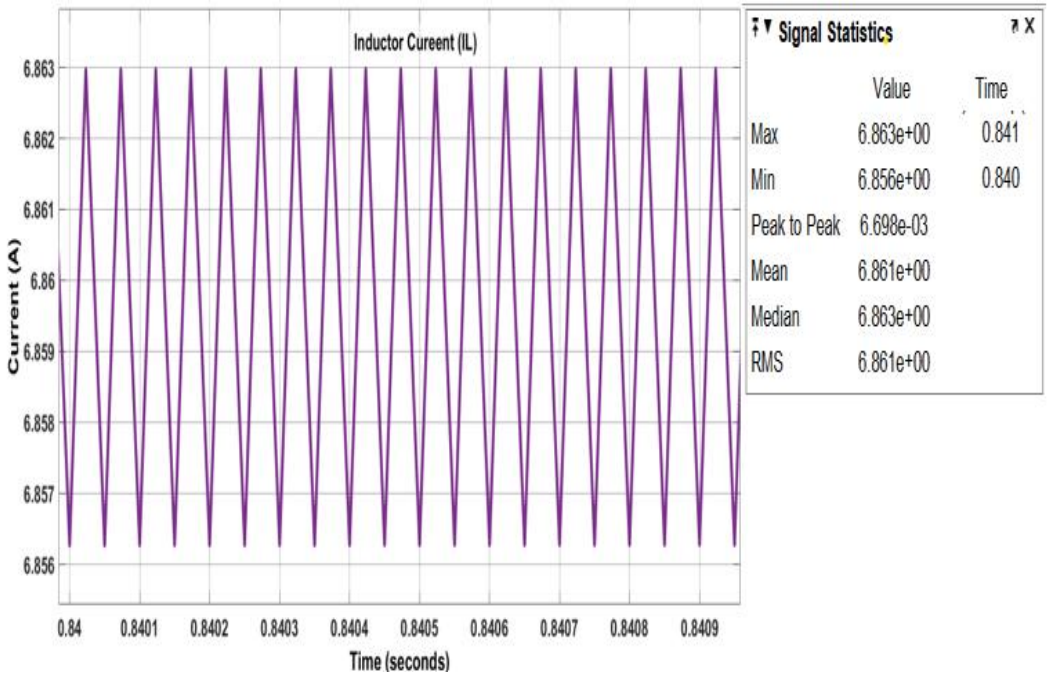


Figure 4.4: Inductor Current Signal Statistics.

Figure 4.4 provides a more detailed look at the steady-state ripple in the inductor current. This section of the waveform is centered at time 2.4135 seconds. According to the signal statistics, the maximum inductor current is 6.857 A, and the minimum is 6.851 A, giving a peak-to-peak ripple of 0.00669 A (or 6.69 mA). The mean, median, and RMS values are all equal to 6.855 A, which confirms a consistent, well-regulated current through the inductor. To evaluate the quality of this ripple, the ripple percentage can be calculated as: $\text{Ripple\%}=(6.69\times10^{-3}/6.855)\times100\approx0.098\%$. This value is very low, which indicates excellent current stability and well-filtered behaviour. A ripple below 0.1% is highly desirable in power converters, as it reduces core losses and improves output voltage stability. This also proves that the chosen inductor value (0.2045 H) effectively smooths the current as per the design requirements.

4.2.3 Duty Cycle Profile

Figures 4.5 and 4.6 illustrate the behaviour of the PWM (Pulse Width Modulation) signal and the corresponding duty cycle that is generated and adjusted by the PI controller during the simulation. The duty cycle is one of the most important control variables in a DC–DC boost converter. It determines how long the power switch (usually a MOSFET) stays ON during each switching cycle. A properly regulated duty cycle ensures the converter steps up the input voltage to the correct output voltage.

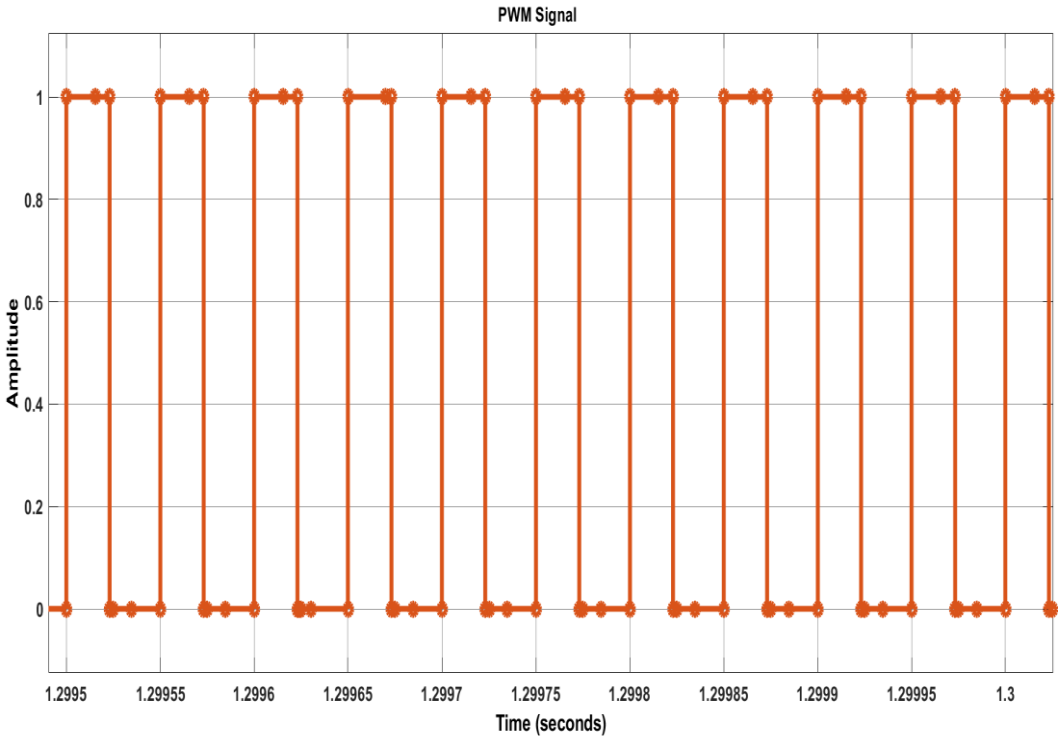


Figure 4.5: Generated PWM signal for MOSFET.

Figure 4.5 shows the actual PWM waveform that is applied to the gate of the MOSFET switch. The signal alternates between 0 and 1, which represent the OFF and ON states of the switch, respectively. This switching happens very rapidly because the converter operates at a switching frequency of 20 kHz. From the graph, it is evident that the switching waveform is regular and stable which confirms that the controller is successfully generating a consistent PWM signal after reaching steady-state. Figure 4.6 shows the duty cycle value being adjusted by the PI controller over the entire 5-second simulation period. At the beginning

(t = 0), the duty cycle starts from zero and begins increasing rapidly as the controller senses the difference between the desired output voltage and the actual output voltage. The controller tries to correct this error by increasing the duty cycle, which turns the switch ON for a longer portion of each switching cycle and causes the output voltage to rise. As the system approaches the target output voltage of 110 V, the duty cycle stabilizes at around 0.4614, which matches the calculated theoretical duty cycle value which was 0.4545 from the design stage.

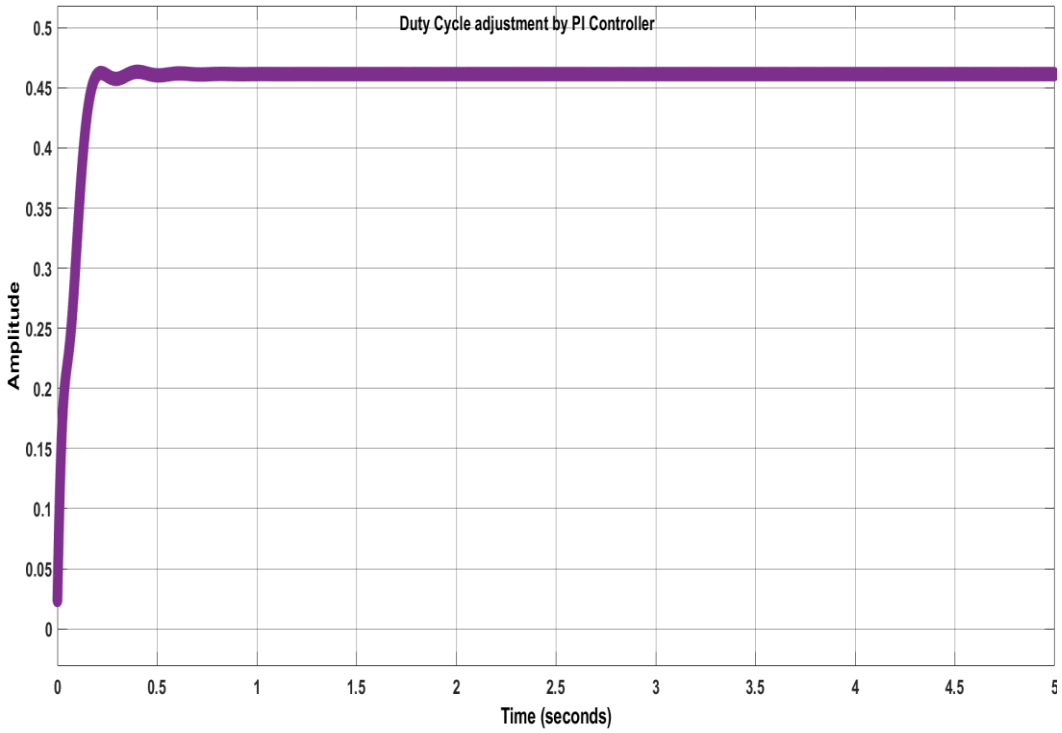


Figure 4.6: Duty Cycle Graph of the Tuned PI controller.

From the duty cycle graph, it is clear that the controller reaches this value very quickly within the first 0.1 seconds and maintains it consistently for the rest of the simulation. The early oscillations in the graph during startup are part of the normal transient response as the controller tunes itself, but these quickly vanish as the output voltage reaches the desired level. This stable and accurate control of the duty cycle is what allows the converter to maintain a constant output voltage, even as load conditions or input voltage attempt to shift the operating

point. The result is a highly efficient and robust system that responds quickly to changes and holds the output steady.

4.3 PERFORMANCE METRICS

To check how accurately the output voltage follows the target value of 110 volts, several error-based performance metrics are calculated. These include IAE, ISE, ITAE, MAE, and MSE. All of these values are taken directly from the simulation and are used to measure the performance of the PI controller over the full 5-second time period. The table 4.2 shows the summary of the performance metrics results. The first value is IAE, which means Integral of

Table 4.2: Summary results of the performance metrics.

Metric	Value
IAE	6.53006
ISE	304.813
ITAE	0.936605
MAE	1.23962
MSE	58.7432

absolute Error. It adds up the total difference between the actual output voltage and the desired voltage, without considering whether the error is positive or negative. The result is 6.53006, which is a low value. This means that the total error over time is small, so the output voltage mostly stayed close to the reference. The second metric is ISE, or Integral of Squared Error. It adds the square of each error over time, so large errors have a bigger impact on the result. The value is 304.813, which is higher than the IAE because it punishes big errors more. This value includes the error during the startup period, where the output voltage overshoots and oscillates slightly before settling. Although this value looks large compared to IAE, it is normal in control systems where quick responses can cause some initial overshoot. The third value is ITAE, which means Integral of Time-weighted Absolute Error. This metric adds more weight to errors that happen later in time. The result is 0.936605, which is very low. This

means that after the converter starts, the output quickly becomes stable and accurate, with very little long-term error. A low ITAE value is a good sign because it means the system does not have long-lasting mistakes or drifting from the reference. Next is MAE, or Mean Absolute Error. This shows the average of all the absolute error values during the simulation. The result is 1.23962 volts, which means the output voltage was on average only about 1.24 volts away from 110 volts. This is quite accurate and shows that the controller works well in keeping the voltage close to the target. Finally, MSE, which is Mean Squared Error, gives the average of all the squared errors. The value is 58.7432, which is affected mostly by the early startup oscillations. This value, although higher than MAE, is expected because it gives more weight to larger differences. In summary, all five error metrics show that the PI controller gives very good performance. The IAE and MAE values are low, showing small average errors. The ITAE is also very low, which proves that the system becomes stable quickly. The ISE and MSE are slightly higher due to the small overshoot and ripple in the early part of the simulation, but they are still within acceptable range. Overall, these results confirm that the PI controller keeps the output voltage close to 110 volts both during startup and steady-state operation.

4.4 IMPACT OF DIFFERENT PARAMETERS IN BOOST CONVERTER

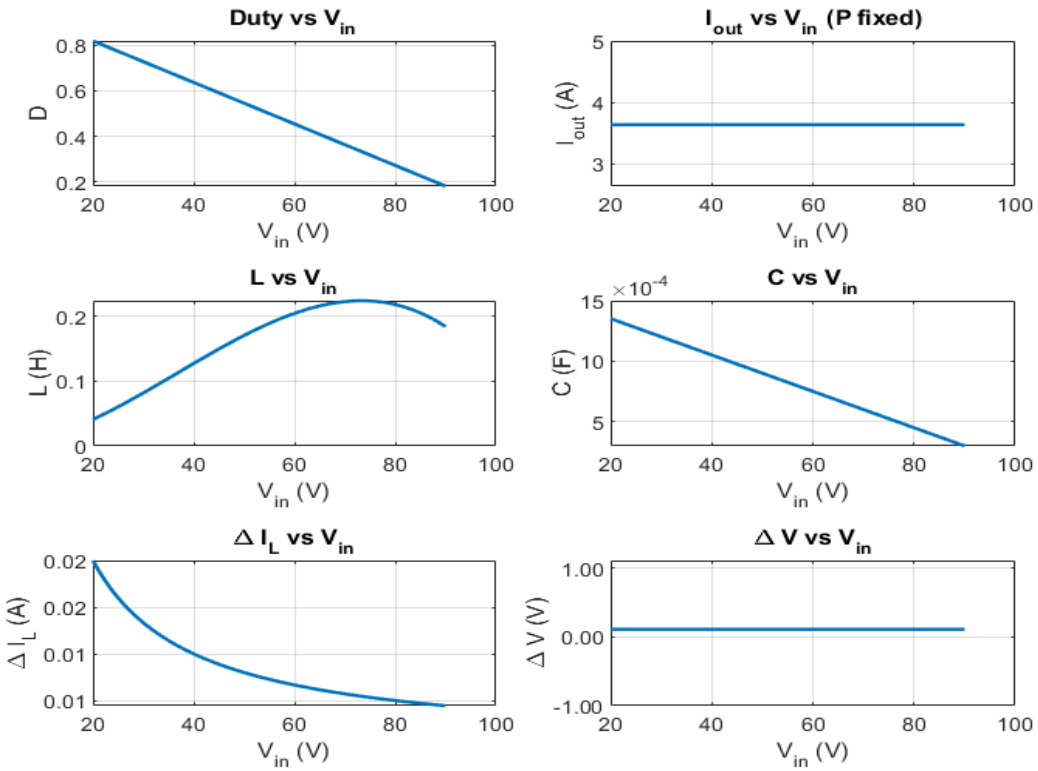


Figure 4.7. Impact of other parameters of boost converter with respect to Vin.

Figure 4.7 shows how the values change when the input voltage Vin increases. As the input voltage increases, the duty cycle drops almost in a straight line. This means the switch needs to stay ON for a shorter time to reach the same output level because the source is already increased. The output current stays nearly flat across the whole range because the output power and output voltage were kept constant. The inductor size shows a "rise-then-fall" trend. At low input voltage the converter needs a larger energy buffer in the inductor, so the required L grows. When the input voltage moves closer to the target output, the step-up effort reduces and the required L begins to come down again. The capacitor value reduces steadily with higher input voltage. With a stronger input, the energy taken from the capacitor each cycle is smaller, so a smaller C can still keep the same voltage quality at the output. The inductor current ripple decreases clearly as input voltage rises; the converter is working less hard to boost, so the current

swings are smaller. The output voltage ripple is basically unchanged across the range because it was designed as a fixed target in this analysis.

Figure 4.8 shows how the converter behaves when the output voltage Vout is increased while the input and power target are unchanged. As Vout rises, the duty cycle increases almost linearly. This tells us the switch must stay ON longer to achieve the higher step-up ratio. At the same time, the output current falls steadily because the same power is delivered at a higher voltage, so less current is needed. A higher conversion ratio demands a larger energy buffer to keep the inductor current swing within the design limit, so a bigger L is selected as Vout goes up. The capacitor value, in contrast, decreases slightly with higher Vout. With the operating point shifting to a higher voltage and lower load current, the charge that the capacitor must supply each cycle is reduced, so a smaller C can still hold the desired output quality. The inductor current ripple stays essentially flat across the whole range as it basically depends on the inductor value. The output voltage ripple increases gradually with Vout as the output voltage ripple are controlled by the capacitance and as capacitance is decreasing so the ripple is increased with increased of output voltage.

Figure 4.8. Impact of other parameters of boost converter with respect to Vout.

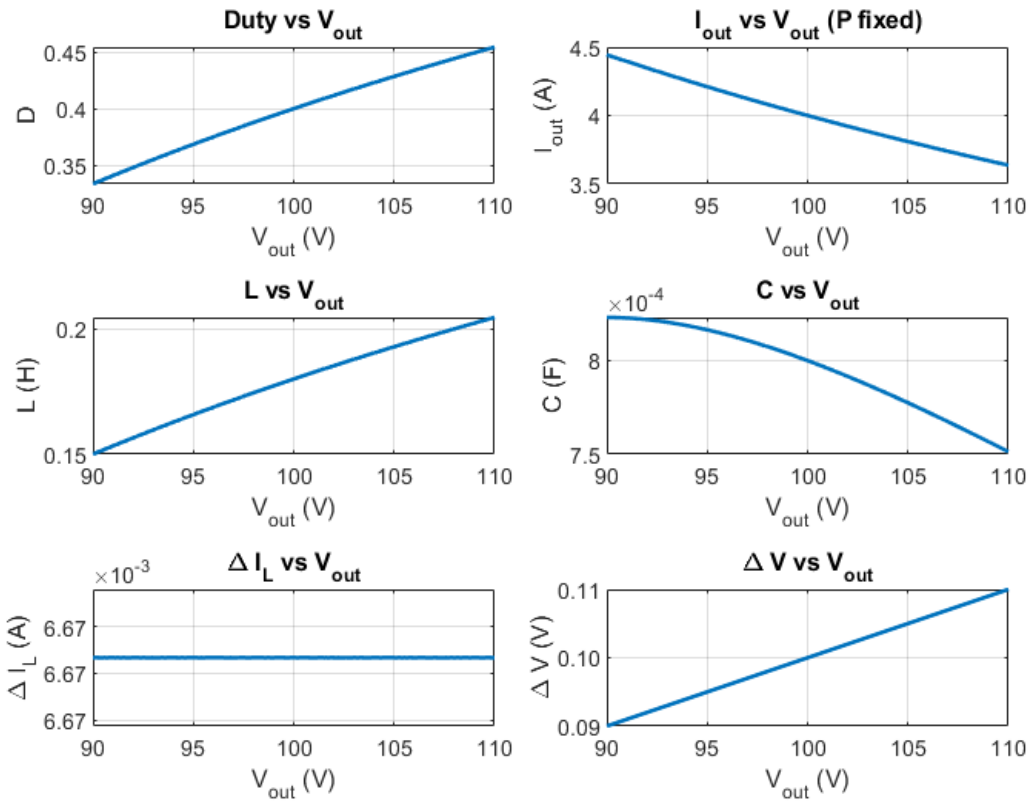


Figure 4.9 shows how the converter responds when the duty ratio D is swept from low to high values. The output voltage rises slowly at small–medium D, then shoots up very sharply as D approaches 1. In this region the converter becomes highly sensitive and tiny changes in duty create very large changes in Vout. The output current decreasing as duty increases as the power is held constant. The required inductor value grows steadily with duty. Higher duty means the inductor must store and release more energy each cycle to maintain the same ripple target, so a larger L is needed. The capacitor increases from low duty to a mid-range peak, then falls off at very high duty. The inductor current ripple remains almost flat across the entire duty range which confirmed that the design target keeps it nearly constant. The output voltage ripple, however, climbs gently at first and then rises sharply near high duty which following the growth of the output voltage as well.

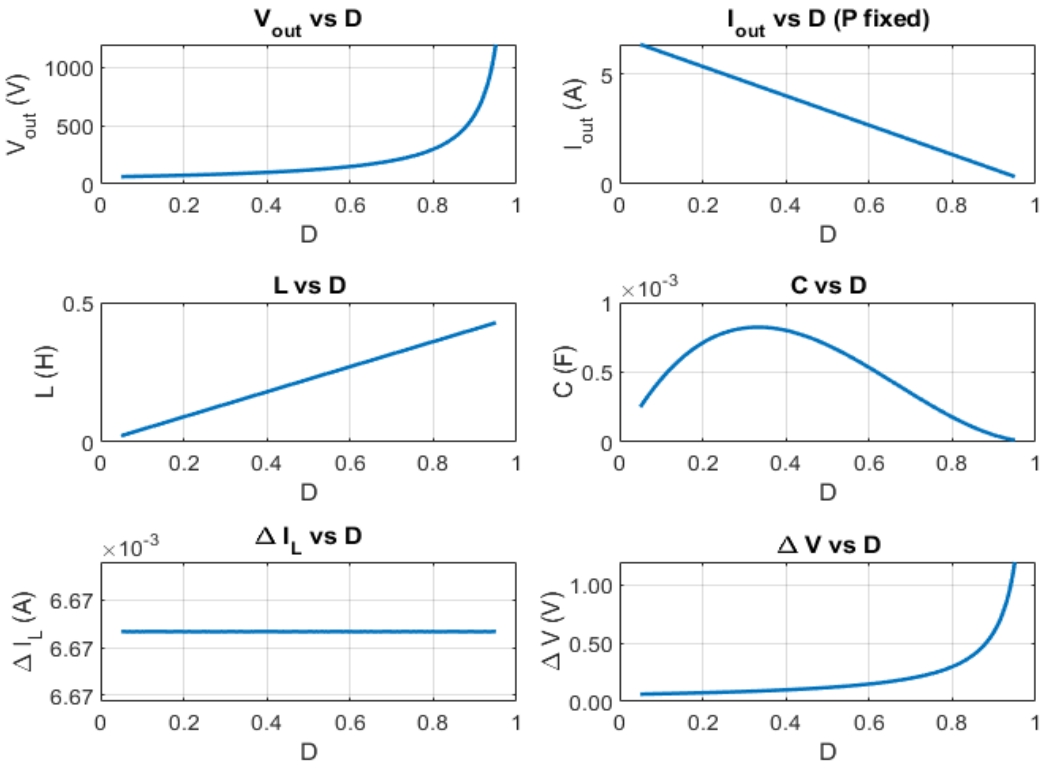


Figure 4.9. Impact of other parameters of boost converter with respect to D.

Figure 4.10 shows how the design values change when the switching frequency fs increases. Both the inductor and the capacitor values drop steeply at low frequency and then level off as frequency gets higher. In simple words, switching faster lets the converter move energy more often each second, so each cycle needs to store less energy and the parts can be smaller. The inductor current ripple and the output voltage ripple are essentially unchanged across the whole frequency range.

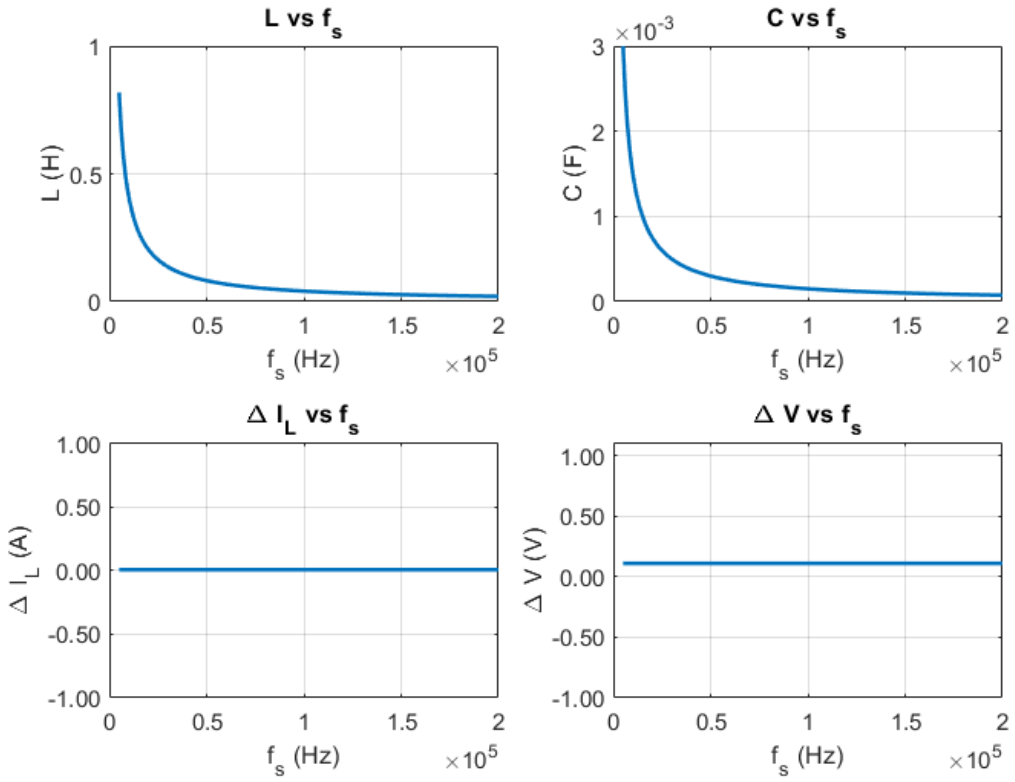


Figure 4.10. Impact of other parameters of boost converter with respect to Fs.

4.5 EFFECT OF INDUCTANCE VARIATION ON SYSTEM PERFORMANCE PARAMETERS

Figure 4.11 examines how changing the inductor value around its nominal point affects the PI-controlled boost converter. The full data of this plot is presented in Table 4.3. The current ripple shows a non-linear pattern: it is highest at the ends of the sweep and smaller near the middle where the inductor smooths the current without making the converter sluggish. Rise time and settling time stay almost unchanged for most values, but both jump sharply at the largest inductance. This means an overly large inductor slows the converter and delays regulation. overshoot is generally moderate but drops to a minimum near the mid-range inductance, then increases again at the edges. The error indices tell a consistent story: IAE, ITAE and ISE climb steadily as inductance increases, while MAE and MSE are lowest near the middle and worsen at the extremes. In simple terms, a bigger inductor makes the system slower and accumulates more error, whereas a too-small inductor lets ripple and overshoot rise. Stability margins

remain acceptable across the sweep. the gain margin is fairly flat but tends to dip at the highest inductance, while the phase margin varies slightly and improves at some points but not enough to offset the slower dynamics.

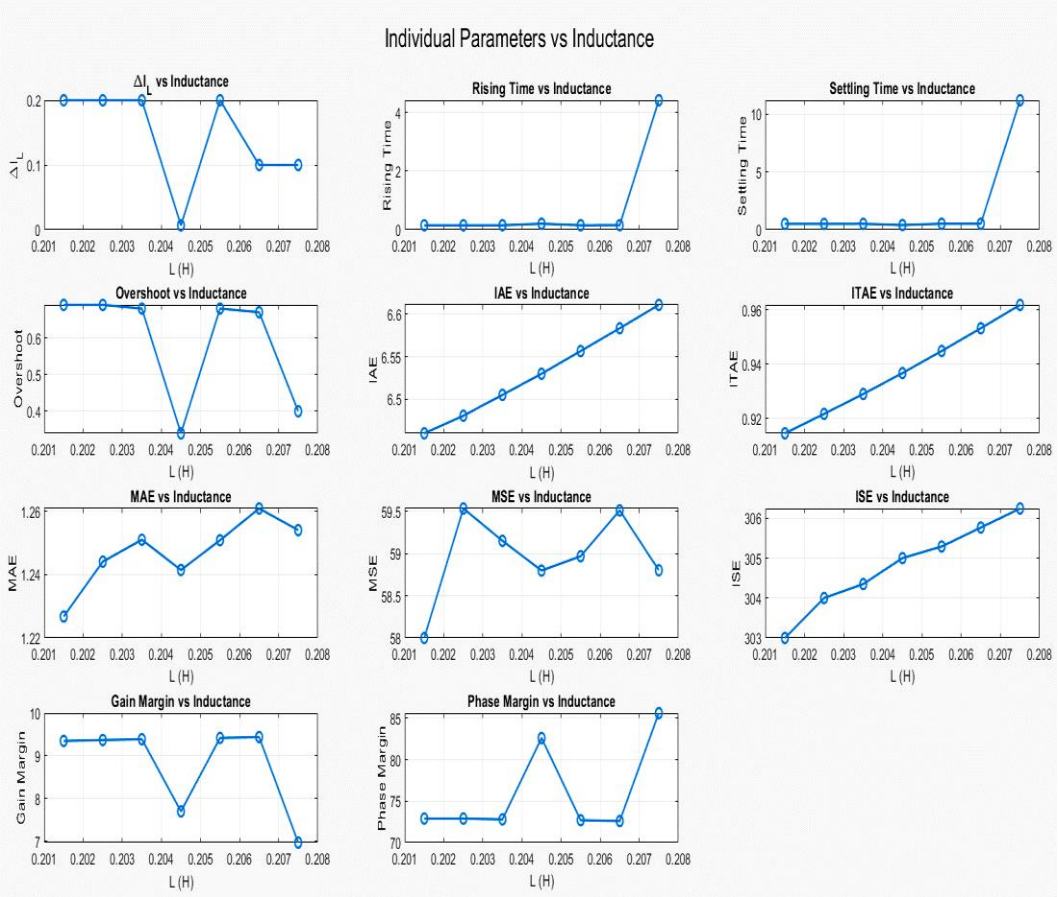


Figure 4.11. Effect of changing inductor on the system performance.

Table 4.3. Data on the impact of inductance variation on boost converter performance

Parameter	Values						
Inductance (H)	0.2015	0.2025	0.2035	0.2045	0.2055	0.2065	0.2075
V_{in} (V)	60	60	60	60	60	60	60
V_{out} (V)	110	110	110	110	110	110	110
Capacitance (F)	7.51E-04	7.51E-04	7.51E-04	7.51E-04	7.51E-04	7.51E-04	7.51E-04
Resistance (Ω)	30.25	30.25	30.25	30.25	30.25	30.25	30.25
Power (W)	400	400	400	400	400	400	400
frequency (Hz)	2.00E+04	2.00E+04	2.00E+04	2.00E+04	2.00E+04	2.00E+04	2.00E+04
Duty cucle	0.4545	0.4545	0.4545	0.4545	0.4545	0.4545	0.4545
I_{outmax} (A)	3.6364	3.6364	3.6364	3.6364	3.6364	3.6364	3.6364
ΔI_L (A)	0.2	0.2	0.2	0.0067	0.2	0.1	0.1
ΔV_{out} (V)	0.11	0.11	0.11	0.11	0.11	0.11	0.11
Rising Time (s)	0.151	0.151	0.152	0.205	0.153	0.154	4.41
Settling Time (s)	0.509	0.512	0.514	0.406	0.519	0.521	11.2
Overshoot (%)	0.69%	0.69%	0.68%	0.34%	0.68%	0.67%	0.40%
IAE	6.46	6.4807	6.5052	6.53	6.55667	6.58345	6.61088
ITAE	0.914491	0.921655	0.928988	0.936685	0.944826	0.953192	0.961794
MAE	1.22678	1.24412	1.25105	1.24148	1.25089	1.26092	1.25408
MSE	5.80E+01	59.5364	59.1529	5.88E+01	58.9701	59.5142	58.8036
ISE	3.03E+02	3.04E+02	304.351	3.05E+02	305.291	305.765	306.242
Kp	0.0239	0.0239	0.0239	0.0239	0.0239	0.0239	0.0239
Ki	8.2608	8.2608	8.2608	8.2608	8.2608	8.2608	8.2608
Gain margin	9.35dB @ 21.6 rad/s	9.37dB@ 21.6 rad/s	9.39dB @ 21.5 rad/s	7.7dB@ 40.8 rad/s	9.42 dB @ 21.3 rad/s	9.44 dB @ 21.2 rad/s	6.97 dB @ 2 rad/s
Phase margin	72.9 deg @ 6.84 rad/s	72.9 deg @ 6.82 rad/s	72.8 deg @ 6.8 rad/s	82.6 deg @ 9.37 rad/s	72.7 deg @ 6.75 rad/s	72.6 deg @ 6.72 rad/s	85.6 deg @ 0.37 rad/s

4.6 EFFECT OF RESISTANCE VARIATION ON SYSTEM PERFORMANCE PARAMETERS

Figure 4.12 studies how changing the load resistance R affects the PI-controlled boost converter. The complete data corresponding to this plot is presented in Table 4.4. The error metrics IAE, ISE, ITAE, MAE, and MSE drop sharply as R increases from the lowest values and reach their best region around the mid-range and beyond this point they shows minor increase. The time responses in Figure 30 tells a consistent story. Rise time is fastest around the mid-range resistance and becomes noticeably slower at the highest RRR. Settling time is fairly steady up to about 25-30 Ω, but it lengthens once the load becomes light and shows slower dynamics. Overshoot is largest at the lowest R, falls quickly with increasing R, then suddenly rise up at 40 Ω and goes to zero again. Stability trends are favourable with higher resistance. phase margin improving as R

increases, indicating a more damped, easier-to-control plant under light load. Gain margin dips around the mid-high R region but remains acceptable and recovers slightly at the top end.

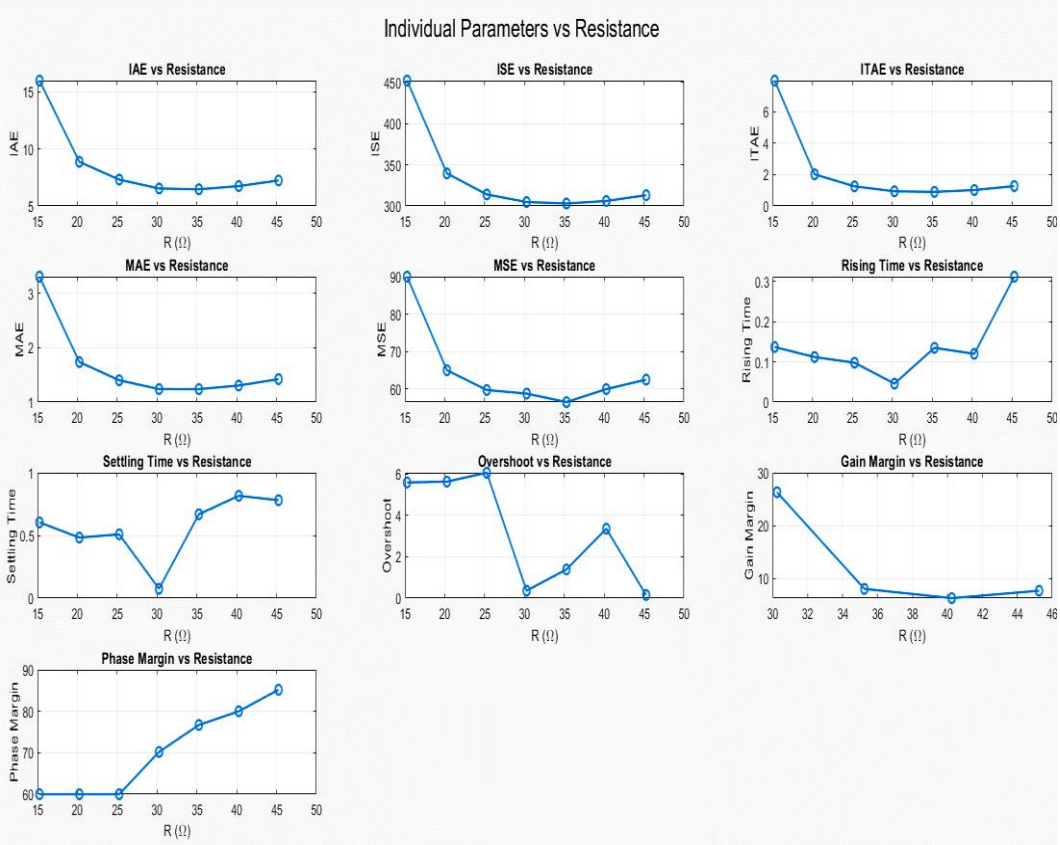


Figure 4.12. Effect of changing resistance on the system performance.

Table 4.4. Data on the impact of resistance variation on boost converter performance

Parameter	**Values**						
Resistance (Ω)	30.25	15.25	20.25	25.25	35.25	40.25	45.25
Inductance (H)	0.2045	0.2045	0.2045	0.2045	0.2045	0.2045	0.2045
Capacitance (μF)	751.31	751.31	751.31	751.31	751.31	751.31	751.31
Power (W)	400	793.44	597.53	479.2	343.262	300	267.4
Frequency (Hz)	20000	20000	20000	20000	20000	20000	20000
I_L (A)	6.851	13.6	10.21	8.196	5.889	5.167	4.605
I_{outmax} (A)	3.6364	3.6364	3.6364	3.6364	3.6364	3.6364	3.6364
ΔI_L	0.0067	0.0067	0.0067	0.0067	0.0067	0.0067	0.0067
ΔV_{out} (V)	0.11	0.11	0.11	0.11	0.11	0.11	0.11
Duty cucle	0.4545	0.4545	0.4545	0.4545	0.4545	0.4545	0.4545
IAE	6.53006	15.9578	8.86206	7.30847	6.46036	6.74075	7.23295
ISE	304.813	452.122	339.579	314.043	303.042	306.072	313.106
ITAE	0.936605	7.99723	2.02207	1.25287	0.899971	1.01776	1.27031
MAE	1.23962	3.30822	1.73659	1.40157	1.23865	1.30491	1.42253
MSE	58.7432	90.0363	65.001	59.7065	56.4758	59.9522	62.4856
V in	60 v	60 v	60 v	60 v	60 v	60 v	60 v
V out	110 v	110.1 v	110.1 v	110.1 v	110.1 v	110.1	110.1
Rising Time (s)	0.0459	0.137 second	0.112 seconds	0.0979 seconds	0.135 seconds	0.12 seconds	0.312 seconds
Settling Time (s)	0.0746	0.604 seconds	0.483 second	0.509 seconds	0.669 seconds	0.816	0.781
Overshoot (%)	0.361	5.60%	5.64%	6.07%	1.39%	3.36%	0.15%
Kp	0.023954	0.51835	0.42765	0.32794	0	0	0
Ki	8.2609	4.6135	5.443	5.9299	3.7072	3.8869	2.8133
Gain margin	26.3	Inf dB @ Inf rad/s	Inf dB @ Inf rad/s	Inf dB @ Inf rad/s	7.99 dB@ 24 red/s	6.23 dB @ 26.4 rad/s	7.64 dB @ 28.5 rad/s
Phase margin	70.2	60 deg @ 10.7 rad/s	60 deg @ 13.3 rad/s	60 deg @ 15.3 rad/s	76.7 deg @ 7.27red/s	80 deg @ 7.67 rad/s	85.2 deg @ 5.34 rad/s

4.7 EFFECT OF CAPACITANCE VARIATION ON SYSTEM PERFORMANCE PARAMETERS

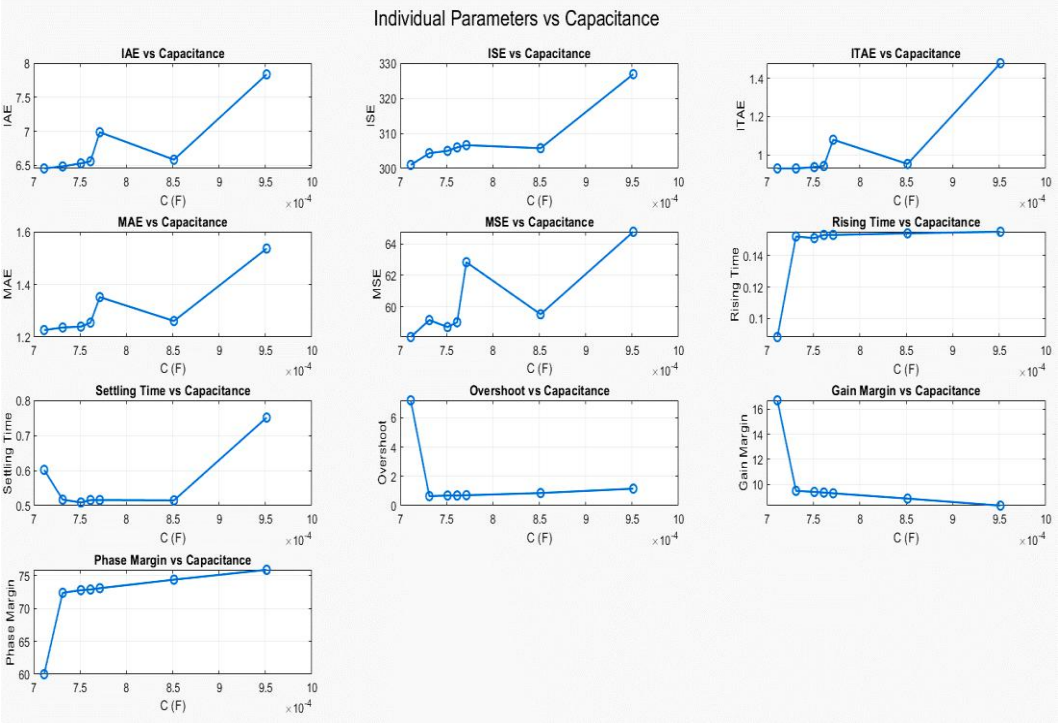


Figure 4.13. Effect of changing capacitance on the system performance.

Figure 4.13 shows how the PI-controlled boost converter behaves when the output capacitor is varied around its nominal value. The complete data corresponding to this plot is presented in Table 4.5. Overshoot is large at the smallest capacitance and then drops to nearly zero for all higher values and increase very slowly. Phase margin also grows slightly with capacitance, so stability improves as the capacitor gets larger. Gain margin stays almost flat, with only a small rise at the upper end, meaning robustness is not very sensitive to this change. Rising time increases gradually with larger C, and settling time stays short for moderate values but becomes noticeably longer at the highest C. The error indices tell the same story. After an initial improvement when we move away from the smallest C, most metrics trend upward as capacitance continues to increase. A very large capacitor makes the loop slower, so the controller accumulates more error even though the response is well damped.

Table 4.5. Data on the impact of capacitance variation on boost converter performance

Parameter	Values						
Capacitance (F)	7.51E-04	0.00071131	0.00073131	0.00076131	0.00077131	0.00085131	0.00095131
V_{in}	60	60	60	60	60	60	60
V_{out}	110.1	110.1	110.1	110.1	110.1	110.1	110.1
Inductance (H)	2.05E-01	2.05E-01	2.05E-01	2.05E-01	2.05E-01	2.05E-01	2.05E-01
Resistance (Ω)	30.25	30.25	30.25	30.25	30.25	30.25	30.25
Power (P)	400	400	400	400	400	400	400
Frequency (Hz)	2.00E+04	2.00E+04	2.00E+04	2.00E+04	2.00E+04	2.00E+04	2.00E+04
Duty cycle	0.4545	0.4545	0.4545	0.4545	0.4545	0.4545	0.4545
I_L (A)	6.851	6.851	6.851	6.851	6.851	6.851	6.851
I_{outmax} (A)	3.6364	3.6364	3.6364	3.6364	3.6364	3.6364	3.6364
ΔI_L (A)	0.0067	0.0067	0.0067	0.0067	0.0067	0.0067	0.0067
ΔV_{out} (V)	0.11	0.11	0.11	0.11	0.11	0.11	0.11
Rising Time (s)	0.151	0.0883	0.152	0.153	0.153	0.154	0.155
Settling Time (s)	0.509	0.602	0.517	0.516	0.516	0.515	0.751
Overshoot (%)	0.69%	7.20%	0.65%	0.69%	0.71%	0.86%	1.16%
IAE	6.53E+00	6.45494	6.4845	6.56E+00	6.98637	6.58345	7.83626
ITAE	0.9366	0.929826	0.929839	0.942445	1.07959	0.953192	1.47846
MAE	1.2396	1.22647	1.2362	1.25456	1.3517	1.26092	1.53635
MSE	5.87E+01	58.0624	59.144	5.90E+01	62.8366	59.5142	64.778
ISE	3.05E+02	3.01E+02	304.351	3.06E+02	306.639	305.765	326.873
Kp	0.023954	0.0239	0.0239	0.0239	0.0239	0.0239	0.0239
Ki	8.2609	8.2609	8.2609	8.2609	8.2609	8.2609	8.2609
Gain margin	9.41 dB @ 21.4 rad/s	16.7 dB @ 43.2 rad/s	9.5 dB @ 21.4 rad/s	9.36 dB @ 21.4 rad/s	9.3 dB @ 21.3 rad/s	8.88 dB @ 21.2 rad/s	8.32 dB @ 20.9 rad/s
Phase margin	72.8 deg @ 6.77 rad/s	60 deg @ 17.1 rad/s	72.4 deg @ 6.81 rad/s	72.9 deg @ 6.75 rad/s	73.1 deg @ 6.73 rad/s	74.4 deg @ 6.58 rad/s	75.9 deg @ 6.4 rad/s

4.8 EFFECT OF FREQUENCY VARIATION ON SYSTEM PERFORMANCE PARAMETERS

Table 4.3 represents the data on the Impact of Frequency Variation on Boost Converter Performance. Based on this data, Figure 4.14 explores how the controller behaves when the switching frequency is swept from 10 kHz to 90 kHz. Most tracking-error measures (IAE, ISE, ITAE) gradually get better as frequency increases, showing that a faster update of energy per cycle helps the loop follow the reference more closely. MAE and MSE show small bumps, but after the 20–30 kHz region they trend slightly downward and stay fairly stable. Rise time has a clear dip around ~20 kHz (fastest response) and then levels off to a nearly constant value for higher frequencies. Settling time shows the same pattern

shorter near ~20 kHz and almost unchanged beyond that. Overshoot is minimal around ~20 kHz and remains very small afterward, confirming good

Table 4.6. Data on the Impact of Frequency Variation on Boost Converter Performance.

Parameter	**Values**						
Frequency (Hz)	20000	10000	15000	30000	45000	60000	90000
Resistance (Ω)	30.25	30.25	30.25	30.25	30.25	30.25	30.25
Inductance (H)	0.2045	0.2045	0.2045	0.2045	0.2045	0.2045	0.2045
Capacitance (μF)	751.31	751.31	751.31	751.31	751.31	751.31	751.31
Power (W)	400	400	400	400	400	400	400
I_L (A)	6.851	6.851	6.851	6.851	6.851	6.851	6.851
I_{outmax} (A)	3.6364	3.6364	3.6364	3.6364	3.6364	3.6364	3.6364
ΔI_L (A)	0.0067	0.0067	0.0067	0.0067	0.0067	0.0067	0.0067
ΔV_{out} (V)	0.11	0.11	0.11	0.11	0.11	0.11	0.11
Duty cycle	0.4545	0.4545	0.4545	0.4545	0.4545	0.4545	0.4545
IAE	6.53006	6.64395	6.58072	6.48051	6.44776	6.43099	6.41525
ISE	304.813	304.824	304.817	304.81	304.809	304.809	304.809
ITAE	0.936605	1.25921	1.08235	0.793541	0.69709	0.646839	0.599918
MAE	1.23962	1.20289	1.27083	1.23459	1.21821	1.22772	1.206
MSE	58.7432	53.9714	57.7381	58.1422	57.8406	58.8282	58.0284
Vin (V)	60 v	60 v	60 v	60 v	60 v	60 v	60 v
Vout (V)	110 v	110.1 v	110.1 v	110.1 v	110.1 v	110.1	110.1
Rising Time (s)	0.0459	0.153 second	0.153 seconds	0.153 seconds	0.153 seconds	0.153 seconds	0.153 seconds
Settling Time (s)	0.0746	0.516 seconds	0.516 second	0.517 seconds	0.517 seconds	0.517	0.517
Overshoot (%)	0.361	0.68%	0.68%	0.68%	0.68%	0.68%	0.68%
Kp	0.023954	0.023954	0.023954	0.023954	0.023954	0.023954	0.023954
Ki	8.2609	8.2609	8.2609	8.2609	8.2609	8.2609	8.2609
Gain margin	26.3	9.41 dB @ 21.4 rad/s	9.41 dB @ 21.4 rad/s	9.41 dB @ 21.4 rad/s	9.41 dB @ 21.4 rad/s	9.41 dB @ 21.4 rad/s	9.41 dB @ 21.4 rad/s
Phase margin	70.2	72.7 deg @ 6.77 rad/s	72.8 deg @ 6.77 rad/s	72.8 deg @ 6.77 rad/s	72.8 deg @ 6.77 rad/s	72.8 deg @ 6.77 rad/s	72.8 deg @ 6.77 rad/s

damping in that region. phase margin consistently high with only a small notch near ~20 kHz, while gain margin exhibits a brief peak around ~20 kHz and then sits close to a steady, acceptable level at higher frequencies.

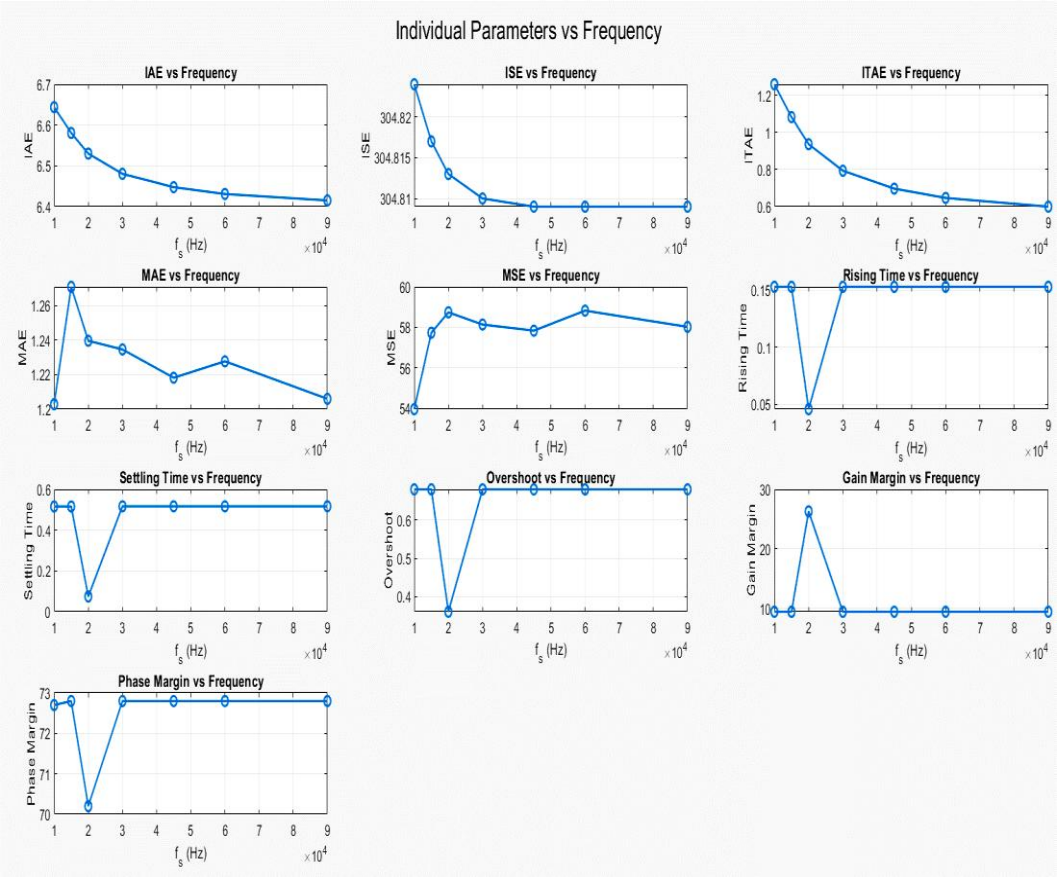


Figure 4.14. Effect of changing frequency on the system performance.

4.9 SUMMARY

In this chapter, the performance of the designed DC–DC boost converter using a PI controller has been analyzed through detailed simulation results. First, the final tuned values of the PI controller were shown, where the proportional gain Kp=0.023954 and the integral gain Ki=8.2609 provided fast and stable response. The output voltage waveform confirmed that the converter successfully stepped up the input voltage from 60 V to a regulated 110 V with a fast rise time of 0.0459 seconds and a quick settling time of 0.0746 seconds. The overshoot was very small at 0.361%, and the ripple was within 0.1%, meeting the design goals. The inductor current profile showed that the converter operated in continuous conduction mode (CCM) as planned. It stabilized around 6.85 A with very low ripple of only 6.69 mA. The duty cycle waveform also proved that the PI controller adjusted the pulse width correctly, quickly settling to a steady value

of 0.4614 which matches approximately with the theoretical calculation. The error-based performance metrics, including IAE, ISE, ITAE, MAE, and MSE, were calculated and analyzed. All values were found to be low and within acceptable limits. These metrics have confirmed that the PI controller is maintained high accuracy throughout the simulation with having the minimal deviation from the reference voltage. So, the results in this chapter have clearly showed that the PI controller was properly tuned. Additionally, the impact of different parameters in boost converter and on the system performance are described with output results.

Chapter 5: CONCLUSIONS

5.1 KEY FINDINGS

This study successfully designed, simulated and analysed the DC–DC boost converter using PI controller in MATLAB/Simulink. The main goal was to regulate the output voltage at 110 V from a 60 V input. After the proper tuning, the PI controller have showed excellent performance with a fast rise time of 0.0459 seconds and a short settling time of 0.0746 seconds. The system had showed a very low overshoot of 0.361% and also output ripple remained within 0.1% which meeting the design targets. The duty cycle quickly settled at 0.4545, which matches the theoretical value. The inductor current remained stable around 6.85 A without falling to zero, confirming continuous conduction mode (CCM). Error-based metrics such as IAE = 6.53, ITAE = 0.93, and MAE = 1.24 further showed that the controller accurately followed the reference voltage. These results prove that the PI controller was properly tuned and provided fast, stable, and accurate voltage regulation.

5.2 LIMITATION OF THE STUDY

Although the simulation results were promising, this study has several limitations. The project was carried out entirely in a simulation environment using MATLAB/Simulink, so no hardware testing was done. Practical factors like switching losses, parasitic elements, heat dissipation, and real-time noise were not included. The converter was assumed to operate in continuous conduction mode only. Also, temperature effects, component tolerance variations, and long-term aging of parts were not considered, which may affect real-world performance.

5.3 PRACTICAL IMPLICATION

The findings of this study have important applications in real-world systems where stable voltage regulation is critical. This includes renewable energy systems like solar panels, battery-powered devices, electric vehicles, and DC microgrids. A well-tuned PI-controlled boost converter ensures efficient power delivery, reduces stress on connected devices, and improves system reliability. The simplicity and effectiveness of the PI controller make it a practical solution for embedded controllers in commercial products. The modeling and tuning approach demonstrated here can help engineers design similar converters for other voltage and power levels with confidence.

5.4 RECOMMENDATION FOR FURTHER STUDY

For future work, it is recommended to implement the same boost converter in hardware to validate the simulation results. Experiments can be done using microcontrollers like Arduino, STM32, or DSPs to test real-time performance and controller response. Further improvement can be explored by applying more advanced control techniques such as fuzzy logic, PID with feedforward control, or artificial intelligence–based tuning methods. Additional studies can also include analysis under discontinuous conduction mode (DCM), effects of component non-idealities, and operation under different load conditions. Optimizing the converter for better efficiency, thermal performance, and EMI reduction can also be future goals.

Bibliography

[1] F. A. Himmelstoss, A. R. Derin, and M. Cernat, “Boost converter with active snubber network,” *Advances in Electrical and Computer Engineering*, vol. 17, no. 1, pp. 55–60, 2017, doi: 10.4316/AECE.2017.01008.

[2] S. D. Tavakoli, G. Kadkhodaei, M. Hamzeh, and K. Sheshyekani, “Non-linear time-delay controller for dc/dc power converters in application of electric vehicles,” *IET Electrical Systems in Transportation*, vol. 7, no. 4, pp. 303–309, Dec. 2017, doi: 10.1049/IET-EST.2017.0005.

[3] J. H. Lee, J. S. Lee, and K. B. Lee, “Current Sensorless MPPT Control Method for Dual-Mode PV Module-Type Interleaved Flyback Inverters,” *Journal of Power Electronics*, vol. 15, no. 1, pp. 54–64, 2015, doi: 10.6113/JPE.2015.15.1.54.

[4] J. T. Su and C. W. Liu, “Gain scheduling control scheme for improved transient response of DC/DC converters,” *IET Power Electronics*, vol. 5, no. 6, pp. 678–692, Jul. 2012, doi: 10.1049/IET-PEL.2010.0313.

[5] R. Priewasser, M. Agostinelli, C. Unterrieder, S. Marsili, and M. Huemer, “Modeling, control, and implementation of DC-DC converters for variable frequency operation,” *IEEE Trans Power Electron*, vol. 29, no. 1, pp. 287–301, 2014, doi: 10.1109/TPEL.2013.2248751.

[6] R. S. R. Babu, S. Deepa, and S. Jothivel, “A closed loop control of quadratic boost converter using PID-controller,” *International Journal of Engineering, Transactions B: Applications*, vol. 27, no. 11, pp. 1653–1662, Nov. 2014, doi: 10.5829/IDOSI.IJE.2014.27.11B.02.

[7] S. Ang, A. Oliva, G. Griffiths, and R. Harrison, *Power-switching converters*. 2010. Accessed: Jul. 17, 2025. [Online]. Available: https://books.google.com/books?hl=en&lr=&id=JUFZDwAAQBAJ&oi=fnd&pg=PP1&dq=Power-Switching+Converters+Ang+Oliva&ots=f5b4sAiwxG&sig=B83P4lRHEiCAMOvhCFvc0-zd6AM

[8] M. Biglarbegian, *Control systems engineering*. 2019. Accessed: Jul. 17, 2025. [Online]. Available: https://books.google.com/books?hl=en&lr=&id=fj6MEAAAQBAJ&oi=fnd&pg=PR9&dq=Control+Systems+Engineering+Nise&ots=HmBDrAFT4d&sig=NyeRpfRePElsyRbY_-g8pYRhGEM

[9] “Power Electronics Converters Applications and Design Mohan - Google Scholar.” Accessed: Jul. 17, 2025. [Online]. Available: https://scholar.google.com/scholar?q=Power+Electronics+Converters+Applications+and+Design+Mohan

[10] R. Erickson and D. Maksimovic, *Fundamentals of power electronics*. 2007. Accessed: Jul. 17, 2025. [Online]. Available: https://books.google.com/books?hl=en&lr=&id=B4XhBwAAQBAJ&oi=fnd&pg=PR19&dq=Fundamentals+of+Power+Electronics+Erickson+Maksimovic&ots=jzv-eEyc2v&sig=T-eU60Pyvb-Dv2xI4A9tv2y0eZc

[11] M. Kazimierczuk, *Pulse-width modulated DC-DC power converters*. 2015. Accessed: Jul. 17, 2025. [Online]. Available: https://books.google.com/books?hl=en&lr=&id=_vgwBgAAQBAJ&oi=fnd&pg=

PR21&dq=Pulse-Width+Modulated+DC-DC+Power+Converters+Kazimierczuk&ots=Wk83jzumkR&sig=yPjXpkZ5qDNekRs1hW59H9rDmo4

[12] R. Mohajery, H. Shayeghi, J. V.-I. J. on, and undefined 2021, "PSO-TVAC based optimized FOPID controller for cascaded DC-DC boost converter," *iotpe.comR Mohajery, H Shayeghi, JL VillanuevaInternational Journal on Technical and Physical Problems of Engineering (IJTPE), 2021•iotpe.com*, vol. 49, pp. 139–146, 2021, Accessed: Jul. 17, 2025. [Online]. Available: https://www.iotpe.com/IJTPE/IJTPE-2021/IJTPE-Issue49-Vol13-No4-Dec2021/22-IJTPE-Issue49-Vol13-No4-Dec2021-pp139-146.pdf

[13] J. Ahmad *et al.*, "A New High-Gain DC-DC Converter with Continuous Input Current for DC Microgrid Applications," *Energies 2021, Vol. 14, Page 2629*, vol. 14, no. 9, p. 2629, May 2021, doi: 10.3390/EN14092629.

[14] K. Prithivi, M. Sathyapriya, and L. A. Kumar, "Output Voltage Ripple (OVR) Reduction of Boost Converter Using Particle Swarm Optimization," *Circuits and Systems*, vol. 07, no. 12, pp. 4009–4023, 2016, doi: 10.4236/CS.2016.712332.

[15] O. Fatih Kececioglu, A. Gani, and M. Sekkeli, "Design and Hardware Implementation Based on Hybrid Structure for MPPT of PV System Using an Interval Type-2 TSK Fuzzy Logic Controller," *Energies 2020, Vol. 13, Page 1842*, vol. 13, no. 7, p. 1842, Apr. 2020, doi: 10.3390/EN13071842.

[16] M. A. Shahid *et al.*, "Artificial intelligence-based controller for DC-Dc flyback converter," *Applied Sciences (Switzerland)*, vol. 9, no. 23, Dec. 2019, doi: 10.3390/APP9235108.

[17] G. Seshagiri Rao, S. Raghu, and N. Rajasekaran, "Design of feedback controller for boost converter using optimization technique," *International Journal of Power Electronics and Drive Systems*, vol. 3, no. 1, pp. 117–128, Mar. 2013, doi: 10.11591/IJPEDS.V3I1.1737.

[18] A. Marahatta, Y. Rajbhandari, A. Shrestha, S. Phuyal, A. Thapa, and P. Korba, "Model predictive control of DC/DC boost converter with reinforcement learning," *Heliyon*, vol. 8, no. 11, Nov. 2022, doi: 10.1016/J.HELIYON.2022.E11416.

[19] Mirza Fuad Adnan, Mohammad Abdul Moin Oninda, Mirza Muntasir Nishat, and Nafiul Islam, "Design and Simulation of a DC - DC Boost Converter with PID Controller for Enhanced Performance," *International Journal of Engineering Research and*, vol. V6, no. 09, Sep. 2017, doi: 10.17577/IJERTV6IS090029.

[20] A. Daraz, A. Basit, and G. Zhang, "Performance analysis of PID controller and fuzzy logic controller for DC-DC boost converter," *PLoS One*, vol. 18, no. 10, p. e0281122, Oct. 2023, doi: 10.1371/JOURNAL.PONE.0281122.

[21] A. ul Ayesha and Dr. D. R, "Closed Loop Control of an Isolated semi-SEPIC DC-DC Converter using PID Controller," *International Journal of Recent Technology and Engineering (IJRTE)*, vol. 9, no. 2, pp. 1165–1169, Jul. 2020, doi: 10.35940/IJRTE.B4132.079220.

[22] N. F. Nanyan, M. A. Ahmad, and B. Hekimoğlu, "Optimal PID controller for the DC-DC buck converter using the improved sine cosine algorithm," *Results in Control and Optimization*, vol. 14, Mar. 2024, doi: 10.1016/J.RICO.2023.100352.

[23] N. Kunjittipong, S. K.-2024 12th I. Electrical, and undefined 2024, "The PI Control for a Boost Derived Hybrid Converter to Supply DC and AC Loads," *ieeexplore.ieee.orgN Kunjittipong, S Khwan-on2024 12th International Electrical Engineering Congress (iEECON), 2024•ieeexplore.ieee.org*, Accessed:

Jul. 17, 2025. [Online]. Available: https://ieeexplore.ieee.org/abstract/document/10537838/

[24] H. Shayeghi, R. Mohajery, … N. B.-2022 14th, and undefined 2022, "Implementation of PD-PI controller for boost converter using GWO algorithm," *ieeexplore.ieee.orgH Shayeghi, R Mohajery, N Bizon, P Thounthong, N Takorabet2022 14th International Conference on Electronics, Computers and, 2022•ieeexplore.ieee.org*, Accessed: Jul. 17, 2025. [Online]. Available: https://ieeexplore.ieee.org/abstract/document/9847509/

[25] F. P. Priya and K. Latha, "Feedback Linearization Control of Boost Converter," *2019 2nd International Conference on Intelligent Computing, Instrumentation and Control Technologies, ICICICT 2019*, pp. 169–173, Jul. 2019, doi: 10.1109/ICICICT46008.2019.8993341.

[26] K. Sasikala and R. Krishna Kumar, "Design and analysis of boost DC-DC converter with PI controller," *International Journal of Recent Technology and Engineering*, vol. 8, no. 3, pp. 6213–6216, Sep. 2019, doi: 10.35940/IJRTE.C5711.098319.

[27] C. S. Sachin and S. G. Nayak, "Design and simulation for sliding mode control in DC-DC boost converter," *Proceedings of the 2nd International Conference on Communication and Electronics Systems, ICCES 2017*, vol. 2018-January, pp. 440–445, Jul. 2017, doi: 10.1109/CESYS.2017.8321317.

[28] M. Shadoul, R. Al Abri, H. Yousef, and M. Masoud, "DC- DC boost converter controller design for PV applications," *2017 9th IEEE-GCC Conference and Exhibition, GCCCE 2017*, Aug. 2018, doi: 10.1109/IEEEGCC.2017.8448164.

[29] K. Ullah *et al.*, "Design of dual loop controller for boost converter based on PI controller," *pubs.aip.org*, vol. 14, no. 2, Feb. 2024, doi: 10.1063/5.0191079.

[30] D. Lenine, C. Sai Babu, and G. Shankaraiah, "Performance evaluation of fuzzy and PI controller for boost converter with active PFC," *International Journal of Power Electronics and Drive Systems*, vol. 2, no. 4, pp. 445–453, Dec. 2012, doi: 10.11591/IJPEDS.V2I4.522.

[31] O. Rabiaa, B. H. Mouna, S. Lassaad, F. Aymen, and A. Aicha, "Cascade Control Loop of DC-DC Boost Converter Using PI Controller," *International Symposium on Advanced Electrical and Communication Technologies, ISAECT 2018 - Proceedings*, Jan. 2019, doi: 10.1109/ISAECT.2018.8618859.

[32] "Modelling and Simulation of High Gain Hybrid Boost Converter." Accessed: Jul. 17, 2025. [Online]. Available: https://www.researchgate.net/publication/317328294_Modelling_and_Simulation_of_High_Gain_Hybrid_Boost_Converter

[33] G. Arunkumar, C. Dhanamjayulu, … S. P.-I., and undefined 2021, "Implementation of optimization-based PI controller tuning for non-ideal differential boost inverter," *ieeexplore.ieee.orgG Arunkumar, C Dhanamjayulu, S Padmanaban, BR Prusty, B KhanIEEE Access, 2021•ieeexplore.ieee.org*, Accessed: Jul. 17, 2025. [Online]. Available: https://ieeexplore.ieee.org/abstract/document/9398688/

[34] "Rashid, M. H., Power Electronics: Circuits, Devices,... - Google Scholar." Accessed: Jul. 22, 2025. [Online]. Available: https://scholar.google.com/scholar?hl=en&as_sdt=0%2C5&q=Rashid%2C+M.+H.%2C+Power+Electronics%3A+Circuits%2C+Devices%2C+and+Applications%2C+4th+ed.%2C+Pearson%2C+2013.&btnG=

[35] R. Erickson and D. Maksimovic, *Fundamentals of power electronics*. 2007. Accessed: Jul. 22, 2025. [Online]. Available:

https://books.google.com/books?hl=en&lr=&id=B4XhBwAAQBAJ&oi=fnd&pg=PR19&dq=Erickson,+R.+W.,+%26+Maksimovic,+D.,+Fundamentals+of+Power+Electronics,+2nd+ed.,+Springer,+2001.&ots=jzv09wxi3s&sig=dHPNV4IZ5_tEtoGEt_kGyVXU8ss

Appendix

1. MATLAB CODE FOR CALCULATING THE DESIGN PARAMETERS VALUES

```
clc;
P    = 400;       % output power (W)
Vin  = 60;        % input voltage (V)
fs   = 20e3;      % switching frequency (Hz)
Vout = 110;       % output voltage (V)

Ioutmax    = P / Vout       % max output current
ripple_frac = 0.1/100;     % 0.001%:  1e-5

delIL   = ripple_frac * Ioutmax * (Vout / Vin)   % inductor ΔI
delvout = ripple_frac * Vout                     % capacitor ΔV

L = (Vin * (Vout - Vin)) / (delIL * fs * Vout)
C = (Ioutmax * (1 - Vin/Vout))   / (fs * delvout)

R = Vout^2 / P               % load resistance
d = (Vout - Vin) / Vout      % duty cycle
```

2. MALTAB CODE FOR CALCULATING THE PERFORMANCE METRICS VALUES

```
vin_values = out.Vin_Data.signals.values;

vout_values = out.Vout_Data.signals.values;
Vref = 110*ones(size(vout_values));
t = out.Vin_Data.time;

% 1) Form the error signal
e = Vref - vout_values;

% 2) Integrals via trapz
IAE  = trapz(t, abs(e));
ISE  = trapz(t, e.^2);
ITAE = trapz(t, t .* abs(e));

% 3) Time-averages for MAE/MSE
MAE  = mean(abs(e));
MSE  = mean(e.^2);

fprintf('IAE:  %g\nISE:  %g\nITAE: %g\nMAE:  %g\nMSE:  %g\n', IAE, ISE,
ITAE, MAE, MSE);
```